SKB

TECHNICAL REPORT 85-03

Porosities and diffusivities of some non-sorbing species in crystalline rocks

Kristina Skagius
Ivars Neretnieks
The Royal Institute of Technology
Department of Chemical Engineering

Stockholm, 1985-02-07

SVENSK KÄRNBRÄNSLEHANTERING AB
SWEDISH NUCLEAR FUEL AND WASTE MANAGEMENT CO

BOX 5864 S-102 48 STOCKHOLM
TEL 08-67 95 40 TELEX 13108-SKB

POROSITIES OF AND DIFFUSIVITIES OF SOME NON-SORBING SPECIES IN CRYSTALLINE ROCKS

Kristina Skagius, Ivars Neretnieks

Roayal Institute of Technology
Stockholm, Sweden 1985-02-07

POROSITIES OF AND DIFFUSIVITIES OF SOME NON-SORBING SPECIES IN CRYSTALLINE ROCKS

Kristina Skagius, Ivars Neretnieks

1985-02-07

SUMMARY

The diffusion of non-sorbing species in different rock materials and fissure coating materials has been studied on a laboratory scale. The non-sorbing species were iodide, Uranine and Cr-EDTA. The results show that the effective diffusivity of iodide in rock materials with fissure coating material is of the same magnitude or higher than the effective diffusivity of iodide in rock materials without fissure coating material. The results also show that it is not possible to give one value of the diffusivity in a rock material from a certain area. The variations in the rock material are too large. The estimated effective diffusivity of iodide in rock materials without fissure coating material was found to be in the range $1 \cdot 10^{-14}$ m^2/s to $70 \cdot 10^{-14}$ m^2/s.

The results also emphasize the necessity to distinguish between different porosities. The effective diffusivity is dependent on the "transport" porosity. This means that a higher determined total porosity does not always lead to a higher effective diffusivity.

There are also some indications that the relation between the effective diffusivity of a component in a rock material and the bulk phase diffusivity of the same component is not only depending on the properties of the rock material but also to some extent on the diffusing component.

CONTENTS

INTRODUCTION

An important question related to the nuclear power program is how to dispose of the wastes from the plants in a safe way. In Sweden and many other countries the most interesting alternative is to place the waste in deep underground repositories in crystalline rock. If radionuclides are released from the repository and enter the groundwater they could be transported towards the biosphere by the groundwater flow in the fissure networks within the rock body. The time until the nuclide concentration in the biosphere will reach critical values depends on the groundwater flow but also on the interaction between nuclides and rock.

Besides fissures the rock matrix contains micropores filled with stagnant groundwater. Under naturally prevailing hydraulic gradients the transport by flow in this pore system can be neglected compared to transport by molecular diffusion. This means that diffusion into the micropores in the rock matrix can act as a retarding and diluting mechanism by removing the nuclides from the flowing groundwater in the fissures (1). If the nuclides also are being sorbed on the rock material or react chemically with it this diffusion into the micropores will lead to a reaction or sorption not only at the fissure surfaces but at the micropore surfaces in the rock body as well. This has a profound effect on the retardation of the nuclides.

The fissure surfaces in old fissures, which have been in contact with moving groundwater, may have a different mineral composition than the surrounding rock. This fissure coating material could be the result of weathering and alteration of the rock or precipitates and crystallization products from the groundwater. To estimate the velocity of the nuclides in the groundwater in the fissures it is important to know the sorption (chemical reaction) of the nuclides and the diffusion in micropores in both the fissure coating material and the surrounding rock. This paper describes diffusion experiments with non-sorbing species (iodide, Uranine and Cr-EDTA) in different rock materials and fissure coating materials.

DESCRIPTION OF THE ROCK MATERIALS AND FISSURE COATING MATERIALS

The rock materials were taken from different areas of Sweden, and at different depths. The fissure coating materials were from the Stripa mine in central Sweden and from Finnsjön outside Forsmark on the east coast of Sweden. Table 1 gives the areas and depths from which the rock materials have been taken, and also a description of the materials and a notation that will be used in the presentation of the results from the diffusion experiments.

The fissure coating materials and their description have been received from the Swedish Geological Survey (SGU) in Gothenburg (2), and that of the other rock materials from the SGU in Uppsala (3).

POROSITY DETERMINATION

Two different methods were used to determine the porosity of the rock pieces studied in the diffusion experiments. The first method was a "water saturation" method (method 1) and was made on the pieces before the diffusion experiment was started. The pieces were kept at 90^{o} C in vacuo for three days. The dried pieces were then weighed. After that the pieces were placed above a pan of distilled water in a vacuum chamber. A pressure close to the boiling point of water at ambient temperature (~ 25 m Hg) was maintained for several hours, and then the samples were dropped into the water. After a week the pieces were taken out from the water and the surfaces of the pieces were dried carefully with a piece of paper. Surface dry, the pieces were put on a balance and the weights were registered as a function of time. Figure 1 shows a weight versus time plot for a granitic piece from Finnsjön. The weight extrapolated to time zero, and the weight at the first break of the curve (in this case after about 1.5 minutes) was chosen. From the difference between these two weights and the weight of the dry piece two values of the porosity was calculated. The weight at time zero probably includes a very thin layer of water on the surface, since the evaporation rate from time zero until the first break point of the curve seems to be constant. Then at the first break point of the curve, water starts to evaporate from the pores in the rock piece.

The second method was a leaching method (method 2). The pieces were saturated with a solution of iodide, Uranine or Cr-EDTA of known concentration. The amount of component each piece contained in the saturated condition was determined by leaching out the component from the piece with distilled water. From this information the pore volume and the porosity of the piece were determined. The porosity measurements by the second method were carried out after the diffusion experiments. The results of the porosity determination are presented in Table II.

DIFFUSION EXPERIMENTS

The method used in the diffusion experiments is in principle the same that has been used previously (8) and by other investigators (4, 5, 6, 7). A hole with the same dimension as the piece of the rock, was made in a 10 mm thick PVC-plate. The piece of the rock was fixed in the hole with silicon glue. The plate with the rock sample was then heated in a vacuum chamber and saturated with distilled water by the same method used in making the porosity measurements, the water saturation method. After saturation two chambers made of transparent PVC were fastened on to the PVC-plate, one on each side (see Figure 2). In the experiments with Uranine and Cr-EDTA one of the chambers was filled with distilled water and the other was filled with a solution containing Uranine (~ 10 g/l) or Cr-EDTA (~ 8 g/l). In the first experiments with iodide one chamber was filled with distilled water and the other with a solution containing 1 mol/l of sodium iodide. Later it was shown that there had been some erosion of the rock samples that had been in contact with the 1 mol/l sodium iodide solution. In all the following experiments a solution containing 0.1 mol/l sodium iodide was used instead. To avoid any osmotic effects the other chamber was filled with 0.1 mol/l sodium nitrate solution instead of distilled water, to obtain equal ionic strength on either side of the rock piece.

A test of the diffusion through the PVC-plate and the silicon glue showed that there was no diffusion through the PVC-plate, and that the diffusion through the silicon glue was so small as to be negligible (8).

Samples (10 ml) were taken from the chamber which at the outset contained distilled water or sodium nitrate solution. The concentration of the diffusing component was measured. The iodide concentration was measured using an ion selective electrode, the concentration of Uranine using UV-spectrophotometry and the concentration of Cr-EDTA using atomic absorption spectrometry. Each time a sample was taken out, 10 ml of distilled water or sodium nitrate was added to the chamber to keep the volume in the chamber constant.

Determination of the diffusivity

The rate of change of concentration at a point in a one-dimensional system is given by Fick's second law

$$\frac{\partial c}{\partial t} = D \frac{\partial^2 c}{\partial x^2} \qquad (1)$$

D is the diffusion coefficient. In this case with diffusion in a porous material the apparent diffusion coefficient must be used to account for porosity, tortuosity and sorption effects. The total porosity of the material is here looked upon as the sum of the "transport" porosity and the "storage" porosity. The storage porosity just influences the accumulation in the system. Eq. 1 can then be written

$$(\varepsilon_{tot} + k_d \cdot \rho) \frac{\partial c}{\partial t} = D_p \cdot \varepsilon^+ \frac{\partial^2 c}{\partial x^2} \qquad (2)$$

ε_{tot} = total porosity

ε^+ = "transport" porosity

k_d = sorption coefficient

ρ = density of the material

D_p = pore diffusion coefficient

Comparing eq. 1 and 2 gives

$$D = \frac{D_p \cdot \varepsilon^+}{\varepsilon_{tot} + k_d \cdot \rho} = \frac{D_e}{\alpha} \qquad (3)$$

where $D_e = D_p \cdot \varepsilon^+$ is the effective diffusion coefficient and $\alpha = \varepsilon_{tot} + k_d \cdot \rho$ is a rock capacity factor.

The solution of eq. 2 for the case of diffusion through a porous slab initially at zero concentration, with constant inlet concentration c_1 at $x=0$ and outlet concentration c_2 ($c_2 \ll c_1$) at $x=\ell$ is (9)

$$\frac{c(x,t)}{c_1} = 1 - \frac{x}{\ell} - \frac{2}{\pi} \sum_{n=1}^{\infty} \frac{1}{n} \sin \frac{n\pi x}{\ell} \exp \left(- \frac{D_e \cdot n^2 \pi^2 \cdot t}{\ell^2 \cdot \alpha}\right) \qquad (4)$$

The rate at which the diffusing substance emerges from a unit area of the face $x=\ell$ of the slab is given by differentiating eq. 4 and putting it into Fick's first law

$$N = - D_e \frac{\partial c}{\partial x}\Big|_{x=\ell} \qquad (5)$$

By integrating eq. 5 with respect to the time t, the total amount of diffusing substance Q which had passed through the slab in time t is obtained.

$$\frac{Q}{\ell \, c_1} = \frac{D_e \cdot t}{\ell^2} - \frac{\alpha}{6} - \frac{2\alpha}{\pi^2} \sum_{n=1}^{\infty} \frac{(-1)^n}{n^2} \exp \left(- \frac{D_e \cdot n^2 \cdot \pi^2 \cdot t}{\ell^2 \cdot \alpha}\right) \qquad (6)$$

As $t \to \infty$ eq. 6 approaches the linear relation

$$Q = \frac{c_1 \cdot D_e}{\ell} \cdot t - \frac{c_1 \cdot \ell \cdot \alpha}{6} \qquad (7)$$

with the slope $c_1 \cdot D_e/\ell$ and an intercept on the time axis $t = \ell^2 \cdot \alpha / 6 \cdot D_e$.

If the diffusing component is not being sorbed on the material then $\alpha = \varepsilon_{tot}$, which means that the intercept on the time axis gives the total porosity of the material.

If the transport only takes place in the pore water then the relation between the effective diffusivity D_e and the bulk phase diffusivity D_v for a component can formally be written

$$D_e = D_p \cdot \varepsilon^+ = \frac{\varepsilon^+ \cdot \delta_D}{\tau^2} \cdot D_v \qquad (8)$$

where δ_D is the constrictivity and τ the tortuosity of the porous material. Providing no size factors, pore sizes or/and sizes of the diffusing component, influence the diffusion, the formation factor or the diffusibility (7), $\varepsilon^+ \cdot \delta_D / \tau^2$, will only depend on the properties of of the porous material.

RESULTS AND DISCUSSION

In Table II the determined effective diffusivities, D_e, together with the measured porosities of all the samples are presented. D_e is determined from the concentration versus time plot by a linear correlation of the experimental data at longer times. The concentration versus time curve was then simulated by using the determined diffusivity and α = experimental porosity in eq. 6. In those cases where α = experimental porosity does not at all fit the experimental data, a simulation with the α-value from eq. 7 was also performed. The α-values determined from eq. 7 are presented in Table II (P3). The experimental concentration versus time plot together with the theoretical curves (eq. 6) for all the samples are presented in an Appendix to this paper.

In Figures 3, 4 and 5 the concentration versus time for iodide, Uranine and Cr-EDTA diffusion through pieces of migmatite from Studsvik, SV, are shown. For both iodide and Uranine diffusion the theoretical curve (eq. 6) with α = experimental porosity fit the experimental data, while for Cr-EDTA diffusion the fit is bad. According to Figure 5 the α-value (P3) is much lower than the porosity obtained by measurements (P1, P2). Comparing the three theoretical curves in Figure 5 it might seem strange that a lower α-value gives a higher concentration after a fixed time. The explanation to this is that D_e is the same in the three curves, which means that the "transport" porosity is the same. A lower α-value then means a lower storage porosity, which in turn leads to a higher concentration at a fixed time. Since Cr-EDTA is assumed to be non-sorbing, α is just the sum of the "transport" porosity and the storage porosity.

Comparing the α-value (P3) with the experimental porosity obtained by the water-saturation method (P1) in Figure 5 may indicate that just a small amount of the pores are available to the Cr-EDTA. However, the porosity measured by the leaching method (P2) indicates that Cr-EDTA has diffused into almost all the pores. If one instead assumes that some pores are more available and some pores are less available to Cr-EDTA diffusion, the steady-state profile will be build up first in the former type of pores. The diffusion in the less available pores

is much lower. If the less available pores are of the storage pore type, they will not have any observable effect either on the build up of the steady-state profile or on the steady-state profile in the more available pores. If the less available pores are of the type "transport" pores the change between unsteady and steady-state profile in them will probably be overlapped by the steady-state transport in the more available pores. The α-value (P3) would then give the amount of more available pores, and the experimental porosity by the leaching method (P2) would give the total porosity. Determination of the α-value from the concentration versus time curve gives no accurate value due to the way of these experiments are performed. The higher the diffusion transport through the piece is, the more α may vary and still give a good fit to the experimental data. This could be seen in the iodide diffusion experiments with rock materials without fissure coating material. In most cases both the porosity determined by the water saturation method and the porosity determined by the leaching method give rather good fits to the experimental data though the porosities sometimes differ by a factor 2 or 3. However, in almost all cases with Cr-EDTA diffusion and in most cases with Uranine diffusion in rock materials without fissure coating material the α-value from the concentration versus time curve is markedly lower than the measured porosities.

For some samples the diffusivities in Table II are presented within brackets, or they have not been evaluated at all. The reason is that the concentration even after long time was very low with a large scatter between the values, which made it difficult to make a linear correlation of the data.

In the experiment with iodide diffusion through a migmatite piece from Studsvik, SV (Figure 3), the experiment was started with distilled water at the low concentration side. After 130 days sodium nitrate was added to the low concentration side to give ionic strenght equal to ionic strength at the high concentration side (ionic strength = 1.0). After the addition of sodium nitrate the diffusivity increased from $12 \cdot 10^{-14}$ m^2/s to $20 \cdot 10^{-14}$ m^2/s. The lower diffusivity may be the result of an osmotic counter flow of water due to the difference in ionic strength between the high and low concentration side. It may

also simply be the effect of diffusion in a more concentrated solution. In the experiment with iodide diffusion in pieces from Finnsjön, F, where both distilled water and sodium nitrate solution (ionic strength = 0.1) have been used at the low concentration side, the diffusivity was not higher when the ionic strength was equal on either side of the piece. However, here the comparison between unequal and equal ionic strength is made between different pieces.

The rock material from Gideå was fine grained granite, GAA 1, and medium - to coarse grained gneiss, GAA 7. The diffusivity evaluated for the granite is markedly higher than for the gneiss for all three of the diffusing components. Also the porosity of the granite is higher than the porosity of the gneiss. The granite and the gneiss were taken from the same drill core with a difference in depth of about 5 meters. All pieces from Svartboberget were also taken from the same core. The diffusivity and the porosity of the granite, SB 7, and the biotite gneiss, SB 21, are higher than the corresponding parameters for the gneiss, SB 1. This shows the difficulty in giving just one value of the diffusivity in a rock material from a certain area because of the variations in the rock material.

In many of the experiments with diffusion through rock pieces with fissure coating material a change in the slope of the concentration versus time data could be found without any change in the experimental conditions. This is the reason why two values of the diffusivity are given in Table II. An example of this is given in Figure 6 which shows the concentration versus time for iodide diffusion through granite with fissure coating material from Finnsjön, Fi 81. In this case the diffusivity increased during the experiment and in other cases (Fi 83, Fi 85) the diffusivity decreased. No specific explanation could be given to this. It could be the result of changes in the rock material or changes in the chemistry of the pore water during the experiment.

In some experiments the pieces contained both granite and fissure coating material. The fissure coating material was then in contact with the high concentration solution. The diffusivities in Table II for the fissure coating materials are the result of diffusion through two different materials in series, except for SP and Fi 51 which

consisted only fissure coating material. The resistance to diffusion at steady state conditions in a piece containing both fissure coating material and granite is the sum of the resistances in the separate layers. This could be expressed as

$$\frac{\ell_1}{D_{e,1}} + \frac{\ell_2}{D_{e,2}} = \frac{\ell_1 + \ell_2}{D_{e,tot}} \qquad (9)$$

where ℓ_1 and ℓ_2 are the thickness of the layers, $D_{e,1}$ and $D_{e,2}$ are the effective diffusivities in each layer and $D_{e,tot}$ is the total diffusivity in the piece. $D_{e,tot}$ is the value given in Table II, and ℓ_1 and ℓ_2 are known. Assuming that the resistance in one layer is zero gives the largest possible resistance in the other layer and consequently the lowest possible diffusivity in that layer. For the iodide diffusion in Fi 81 the lowest possible diffusivity in the fissure coating material was found to be $4.23 \cdot 10^{-14}$ m^2/s and in the granite $2.27 \cdot 10^{-14}$ m^2/s. Figure 7 shows again the experimental concentration versus time curve for iodide diffusion through Fi 81 and also three theoretical curves for diffusion through a piece containing two layers with different diffusivities and porosities in each layer. The theoretical curves are obtained by solving eq. 2 numerically by a computer program (TRUMP) developed at the Lawrence Livermore laboratories (12). The diffusivities in the two layers are different in the different theoretical curves. However, for each curve the combination of the diffusivities in the two layers satisfies eq. 9. To solve eq. 2 the porosity in each layer is also needed. The total porosity of the piece is

$$\varepsilon_{tot} = \frac{V_1 \cdot \varepsilon_1 + V_2 \cdot \varepsilon_2}{V_1 + V_2} \qquad (10)$$

where V_1 and V_2 are the volumes of the layers, ε_1 and ε_2 are the porosity of each layer and ε_{tot} is the total porosity of the piece. Taking ε_{tot} = 3.30 % (from the water saturation method) and assuming that the granite have a porosity of 0.3 %, the porosity of the fissure coating material from eq. 10 is 4.9 %. With these porosities Figure 7 shows that the best fit to the experimental data is obtained when the diffusivity in the granite is between $2.3 \cdot 10^{-14}$ and $2.5 \cdot 10^{-14}$ m^2/s and

the diffusivity in the fissure coating material is between $4.55 \cdot 10^{-13}$ m^2/s and $29.9 \cdot 10^{-13}$ m^2/s (eq. 9 must be satisfied). Figure 7 also shows that the larger the difference in diffusivity between the two layers the more the α-value from eq. 7 differs from the total porosity of the piece.

In many of the pieces with fissure coating material the diffusivity is very high. Since the pieces are from fracture zones or crushed zones or taken near a fissure it may be that microcracks are present which would increase the through transport. This fact and the fact that the diffusivity is estimated in two different materials simultaneously could explain the large variation in the estimated total diffusivities and the difference between α-values and experimental porosities. Although the diffusing components have been treated as non-sorbing, sorption effects can not be eliminated. Uranine diffusion in many of the pieces with fissure coating material give higher α-values than the experimental porosities which could indicate some sorption.

Table II also gives the formation factor, $\varepsilon^+ \cdot \delta_D / \tau^2$, calculated from eq. 8. The bulk phase diffusivity of iodide, D_V, is $1.6 \cdot 10^{-9}$ m^2/s (10). D_V for Uranine and Cr-EDTA has been estimated by the equation of Hayduk-Laudie (11).

$$D_V = 13.26 \cdot 10^{-5} \cdot \mu^{-1.4} \cdot \tilde{V}^{-0.589} \qquad (11)$$

μ is the viscosity of water at the actual temperature and $\tilde{V}$ is the molal volume of the diffusing component at the boiling point. For Uranine D_V was estimated to $4.5 \cdot 10^{-10}$ m^2/s and for Cr^-EDTA $4.2 \cdot 10^{-10}$ m^2/s. Because of the uncertainty in determining the molal volumes these values are rough estimates.

Comparing the estimated formation factors for all three diffusing components in the same rock material shows that iodide in almost all cases give higher values than Uranine and Cr-EDTA. Klinkenberg (13) has showed that the formation factor for a rock material can be determined by measuring the electrical resistivity in a sample saturated with a high conductivity solution. For Finnsjö granite, F, the formation factor determined by the electrical resistivity method was found

to be $8.3 \cdot 10^{-5}$ - $13 \cdot 10^{-5}$ (14). These values are higher than those determined from the diffusion experiments. The formation factor for gabbro from Vipängen, G, determined from electrical resistivity measurements was found to be $2.2 \cdot 10^{-5}$ - $4.3 \cdot 10^{-5}$ (14). These values are about 100 times higher than the formation factor determined from the iodide diffusion experiments in the gabbro (Table II). The electrical resistivity measurements were not done on the same pieces as the diffusion experiments. The results indicate that the formation factor, as defined in eq. 8, is not only depending on the properties of the rock material but also to some extent on the diffusing component.

The samples from Finnsjön, Fi 88 and Fi 89, are taken at different distances from fissure surfaces. The porosity and diffusivity of iodide were measured to find out if there was any variation with distance from the fissure. Figures 8 and 9 show the experimental porosity versus distance from fissure. Fi 88 shows no obvious variation in porosity with distance from the fissure. For Fi 89 the porosity decreases with distance up to about 80 mm from the fissure, and then remains rather constant or increases slightly. In Figure 10 and 11 the diffusivities of iodide from Table II are plotted versus distance from the fissure. In the samples from Fi 88 and from Fi 89 the diffusivities do not show any obvious dependence on the distance from the fissure. In the samples from Fi 89 which were taken near the fissure where the porosity was higher, one would maybe have expected a higher diffusivity. The experimental porosity is, however, a total porosity value. The diffusivity is dependent only on the "transport" porosity. Thus a higher total porosity does not have to give a higher diffusivity. The "transport" porosity could have about the same value even if the total porosity increases.

In Figure 12 the logarithmic value of the effective diffusivities of iodide in the granites gneisses and fissure coating materials are plotted versus the logarithmic value of the experimental porosities determined by the leaching method (P2), and in Figure 13 versus the logarithmic value of α from eq. 7. Results obtained by Bradbury et al (7) for iodide diffusion in different granites from the United Kingdom

are also presented in the Figures as a comparison. For the granites and the gneisses a linear regression has been made (the lines in the Figures) and the mean values, both logarithmic and arithmetic, of the effective diffusivities, porosities and α-values have been calculated. The logarithmic mean values are marked in the Figures. The effective diffusivity in the granites, logarithmic mean value = $22.0 \cdot 10^{-14}$ m^2/s and arithmetic mean value = $25.2 \cdot 10^{-14}$ m^2/s, is higher than in the gneisses, logarithmic mean value = $5.1 \cdot 10^{-14}$ m^2/s and arithmetic mean value = $9.2 \cdot 10^{-14}$ m^2/s. The mean values of the porosity determined by the leaching method are also higher for the granites, logarithmic = 0.24 % and arithmetic = 0.26 %, than for the gneisses, logarithmic = 0.13 % and arithmetic = 0.15 %. The same holds for the α-value where the granites have a logarithmic mean = 0.29 % and an arithmetic mean = 0.33 % and the gneisses have a logarithmic mean = 0.15 % and an arithmetic mean = 0.29 %. For both granites and gneisses the mean α-values are higher than the mean experimental porosity values.

Figures 12 and 13 show that the effective diffusivity of iodide in the fissure coating materials is of the same order of magnitude or higher as in the granites and the gneisses. Those samples that have an effective diffusivity that is of the same order of magnitude as the granites and the gneisses have, however, higher α-values and much higher porosity values. This could be due to a higher "storage" porosity in the fissure coating material, or to a lower pore diffusivity in the fissure coating material compared with the granites and the gneisses.

CONCLUSIONS

The results from this investigation show that the non-sorbing species iodide, Uranine and Cr-EDTA may be transported through different rock materials by diffusion in the micropores. The effective diffusivity of iodide was found to be in the range of $1 \cdot 10^{-14}$ m^2/s to $70 \cdot 10^{-14}$ m^2/s. The estimated diffusivities showed large differences between granite and gneiss taken from the same drill core. Therefore it is not possible to give one precise value of the diffusivity in a rock material from a certain area. The variations in the rock material are too large.

The results also show that iodide, Uranine and Cr-EDTA are able to diffuse through rock materials with fissure coating material. The total diffusivity in rock + fissure coating material is of the same order of magnitude or higher than in rock without fissure coating material. This means that diffusion can transport species from the moving groundwater in fissures in the rock through the fissure coating material and into the rock matrix.

NOTATION

c	concentration in fluid	mol/l, mg/l
c_1	concentration at the high concentration side	mol/l, mg/l
c_2	concentration at the low concentration side	mol/l, mg/l
D	apparent diffusion coefficient	m^2/s
D_e	effective diffusion coefficient	m^2/s
$D_{e,1}$	effective diffusion coefficient in layer 1	m^2/s
$D_{e,2}$	effective diffusion coefficient in layer 2	m^2/s
$D_{e,tot}$	total effective diffusion coefficient in layer 1 and 2	m^2/s
D_p	pore diffusion coefficient	m^2/s
D_v	diffusion coefficient in bulk phase	m^2/s
k_d	sorption coefficient	m^3/kg
ℓ	thickness or length of a rock-piece	m
ℓ_1	thickness of layer 1	m
ℓ_2	thickness of layer 2	m
N	flowrate of diffusing component	$mol/m^2 \cdot s$, $mg/m^2 \cdot s$
P1	porosity from water saturation method	
P2	porosity from leaching method	
P3	α-value from eq. 7	
Q	total amount of diffusing component which had passed through the piece at time t	mol/m^2, mg/m^2
t	time	seconds, hours, days
V_1	volume of layer 1	m^3
V_2	volume of layer 2	m^3
$\tilde{V}$	molal volume of the diffusing component at the boiling point	cm^3/mol
x	length coordinate	
α	rock capacity factor	
δ_D	constrictivity for diffusion	
ε_1	porosity of layer 1	
ε_2	porosity of layer 2	

ε_{tot}	total porosity	
ε^+	"transport" porosity	
μ	dynamic viscosity of water	Ns/m^2
ρ	density of the solid material	kg/m^3
τ	tortuosity	
$\frac{\varepsilon^+ \cdot \delta_D}{\tau^2}$	formation factor	

REFERENCES

1. Neretnieks I.; Diffusion in the Rock Matrix: An Important Factor in Radionuclide Retardation? J. Geophys. Res., vol 85, 1980.

2. Swedish Geological Survey, Eva-Lena Tullborg, Gothenburg, Sweden.

3. Swedish Geological Survey, Kaj Ahlbom and Erik Gustafsson, Uppsala, Sweden.

4. Garrels R.M., Dreyer R.M., Howland A.L.; Diffusion of Ions through Intergranular Space in Water-Saturated Rocks, Bull. Geol. Soc. Am., vol 60, 1949, p. 1809-1828.

5. Melnyk T.; Diffusion in Crystalline Rock, Atomic Energy of Canada Limited, Technical Record, TR-216, 1983, p. 242.

6. Wadden M.M., Katsube T.J.; Radionuclide Diffusion Rates in Igneous Crystalline Rocks, Chem. Geol., vol 36, 1982, p. 191-214.

7. Bradbury M.H., Lever D., Kinsey D.; Aqueous Phase Diffusion in Crystalline Rock, Scientific Basis for Nuclear Waste Management V, vol 11, 1982, p. 569-578.

8. Skagius K., Neretnieks I.; Diffusion in Crystalline Rocks of some Sorbing and Nonsorbing Species, KBS Technical Report 82-12, 1982.

9. Crank J.; The Mathematics of Diffusion, 2nd ed., Oxford University Press, 1975, p. 50-51.

10. Landolt, Börnstein, 6 Auflage, Band II, Teil 5, Transport phänomenei.

11. Reid R.C., Prausnitz J.M., Sherwood T.K.; The Properties of Gases and Liquids, 3rd ed., Mc Graw-Hill, N.Y., 1977.

12. Edwards A.L.; TRUMP: A Computer Program for Transient and Steady State Temperature Distribution in Multidimensional Systems, National Technical Information Service, National Bureau of Standards, Springfield Va, USA, 1972.

13. Klinkenberg L.J.; Analogy between Diffusion and Electrical Conductivity in Porous Rocks, Geol. Soc. Am. Bull., vol 62, 1951, p. 559.

14. Skagius K., Neretnieks I.; Diffusion in Crystalline Rocks, Scientific Basis for Nuclear Waste Management V, vol 11, 1982, p. 509-518.

Table I: Origin of samples

Area	Depth (m)	Description of the material	Notation
Finnsjön Fi 4	~ 100	granite, quartz-granodiorite; quartz, feldspar, microcline, dark mica, hornblende	F
Stripa	~ 340	granite, quartz-monzonite; quartz, feldspar, microcline, light and dark mica	S
Karlshamn		gneiss	KG
Vipängen		gabbro	G
Studsvik	~ 99	migmatite, granitic origin	SV
Gideå	495-496	granite, finegrained, light grey; quartz, feldspar, light and dark mica	GAA 1
Gideå	500-501	gneiss, medium-to coarsegrained, dark grey; quartz, feldspar, biotite	GAA 7
Svartboberget	503-504	gneiss, fine-to medium grained; plagioclase, garnet, epidote, mica, accessoric silicate mineral	SB 1
Svartboberget	504-504.5	migmatite granite, fine-to medium grained, grey; remains of garnet holding gneiss, newly formed coarsegrained quartz-feldspar	SB 7
Svartboberget	508.7-509.2	garnetholding biotite gneiss; stripes of coarsegrained quartz-feldspar	SB 21
Fjällveden	508-509	biotite gneiss; dark stripes of quartz and biotite, light stripes of quartz and feldspar	FJ
Stripa	~ 340	breccia, crushed grains of quartz and feldspar surrounded by fine grained chlorite and clayminerals.	SP

Table I (cont.)

Area	Depth (m)	Description of the material	Notation
Stripa	~ 340	granite + thin layer (< 1 mm) of fissure coating material containing chlorite, calcite and clay-minerals	SS 1
Stripa	~ 340	breccia, grains of quartz and feldspar surrounded by chlorite and muskovite	SS 2
Finnsjön Fi 8	321.6	granite + thick layer (~ 8 mm) of fissure coating material, calcite	Fi 81
Finnsjön Fi 8	72.0	granite + fissure coating material (~ 4 mm) containing prehnite, chlorite and calcite	Fi 83
Finnsjön Fi 8	163.4	granite + thin layer (< 1 mm) of fissure coating material containing laumontite and zeolite minerals	Fi 85
Finnsjön Fi 4	362.1	crushed zone with fissure coating material (~ 1 mm) containing calcite and laumontite	Fi 41
Finnsjön Fi 5	326	fissure coating material containing calcite and prehnite	Fi 51
Finnsjön Fi 8	294	fissure zone/crushed zone with fissure coating material (5-10 mm) containing calcite, prehnite and laumontite	Fi 87
Finnsjön Fi 7	321	fissure zone with fissure coating material (~ 1 mm) containing calcite, prehnite and chlorite	Fi 71
Finnsjön	114.8-115.3	Younger granite, medium grained, grey	Fi 88
Finnsjön Fi 8	181.0-181.7	Younger granite, fine-to medium grained, grey; quartz, microcline, plagioclase, small amounts of biotite	Fi 89

Table II: Results from porosity and diffusivity determinations

Notation		Porosity % Method 1 P1	Porosity % Method 2 P2	α-value % P3	Effective diffusivity, 10^{-14} m²/s Iodide	Uranine	Cr-EDTA	Formation factor 10^{-5}
F	1	-	0.14	0.30	8.4*			5.2
	2	-	0.11	0.20	7.0*			4.4
	3	-	0.06	0.02		0.22		0.5
	5	0.20-0.21	0.12	0.27	7.1			4.4
	6	0.21-0.23	0.07	0.18	4.1			2.6
	7	0.20-0.21	0.09	0.02		0.53		1.2
	8	0.21-0.22	0.10	0.04			0.62	1.5
S	1	-	0.30	1.05	16*			10.0
	2	-	0.27	0.21	13*			8.1
KG	1	-	0.32	0.74	13*			8.1
	2	-	0.26	0.27	4.8			3.0
G	1	-	-	(0.03)	(0.04)			(0.02)
	2	-	-	(0.13)	(0.09)			(0.06)
SV	1	0.20-0.21	0.17	0.30	12*			7.5
					20			12.5
	2	0.21-0.22	0.18	0.22		2.3		5.1
	3	0.20-0.21	0.16	0.03			0.94	2.2
GAA1	1	0.16-0.17	0.12	0.14	10			6.2
					13			8.1
	2	0.15-0.16	0.11	0.14	9			5.6
					11			6.9
	3	0.15-0.17	0.16	0.11		1.3		2.9
	4	0.18-0.19	0.16	0.12		1.3		2.9
	5	0.18-0.19	0.18	0.04			1.6	3.8
	6	0.17-0.18	0.19	0.08			2.3	5.5

Table II (cont.)

Notation		Porosity % Method 1 P1	Porosity % Method 2 P2	α-value % P3	Effective diffusivity, 10^{-14} m^2/s Iodide	Uranine	Cr-EDTA	Formation factor 10^{-5}
GAA 7	1	0.06-0.08	0.06	(0.006)	(0.58)			(0.36)
	2	0.06	0.07	0.05	1.8			1.12
	3	0.07-0.09	0.08	(0.05)		(0.11)		(0.24)
	4	0.11-0.12	0.11	0.11		0.32		0.71
	5	0.14-0.16	-					
	6	0.07-0.08	0.05					
SB 1	1	0.07	0.07	0.07	1.9			1.19
	2	0.07-0.09	0.07	0.12	3.5			2.19
	3	0.08-0.09	0.12	0.07		0.93		2.07
	4	0.08-0.10	0.11	0.07		0.96		2.13
	5	0.06-0.07	0.11					
	6	0.08	-	(0.05)			(0.15)	(0.36)
SB 7	1	0.20-0.25	0.25	1.14	66			41.2
	2	0.22-0.26	0.33	0.30		6.9		15.3
	3	0.28-0.31	0.36	0.29			4.9	11.7
	4	0.29-0.36	0.29	0.58	34			21.2
	5	0.30-0.34	0.38	0.94		5.2		11.6
	6	0.22-0.26	0.34	0.13			2.9	6.9
	7	0.26-0.30	0.27	0.28	26			16.2
SB 21	1	0.24-0.28	0.32	0.13			2.5	6.0
	2	0.29-0.34	0.21	0.26	15			9.4
	3	0.30-0.35	0.38	0.52		7.8		17.3
	4	0.30-0.34	0.29	0.06			3.0	7.1
	5	0.28-0.32	0.28	0.92	36			22.5
	6	0.23-0.28	0.32	0.62		6.0		13.3

Table II (cont.)

Notation		Porosity % Method 1 P1	Porosity % Method 2 P2	α-value % P3	Effective diffusivity, 10^{-14} m²/s Iodide	Uranine	Cr-EDTA	Formation factor 10^{-5}
FJ	1	0.25-0.26	0.10	0.36	7.2			4.5
	2	0.27-0.29	0.10	0.15	7.4			4.6
	3	0.23-0.24	0.17	0.02		0.36		0.8
	4	0.23-0.24	0.19	0.04		0.39		0.9
	5	0.27-0.28	0.33	0.14			0.81	1.9
	6	0.26-0.28	0.34	0.08			0.60	1.4
SP	1	-	0.41	0.21	0.22*			0.14
	2	-	0.33	0.13	1.4*			0.88
SS 1		-	0.13	1.23	12*			7.5
				1.32	6*			3.75
SS 2	1	-	1.46	1.43	12*			7.5
					22*			13.75
	2	-	0.30	1.10		6.0		13.3
						9.0		20.0
Fi 81	1	2.57-3.30	3.62	0.50	6.5*			4.1
					9.2*			5.75
	2	3.00-3.31	4.55	0.10		1.3		2.9
Fi 83	1	1.90-2.19	1.63	27.5	250*			156.3
					165*			103.1
	2	1.28-1.35	1.57	3.50		6.2		13.8
Fi 85	1	1.10-1.57	1.11	1.05	1900*			1188
					1000*			625
	2	0.78-1.00	0.78	2.50		5.0		11.1

Table II (cont.)

Notation		Porosity % Method 1 P1	Porosity % Method 2 P2	α-value % P3	Effective diffusivity, 10^{-14} m²/s Iodide	Uranine	Cr-EDTA	Formation factor 10^{-5}
Fi 41	1	-	-	24.0	6000*			3750
	2	-	-	24.0		1600		3556
						2000		4444
	3	7.31-7.57	4.20	50.0	2000*			1250
					2500*			1563
	4	7.12-7.49	6.75	8.27		4000		8889
						900		2000
Fi 51	1	1.67-1.83	1.52	1.55	120			75.0
	2	2.67-2.79	3.37	1.30		22		48.9
	3	3.51-3.61	4.27	2.82			48	114.3
Fi 87	1	0.99-1.14	0.89	0.40	3.0			1.9
	2	1.43-1.58	2.46	0.80			1.0	2.4
	3	1.17-1.25	0.88	0.27		0.70		1.6
Fi 71	1	1.47-1.55	0.87	0.50	1.6			1.0
	2	1.67-1.79	1.55	2.80		150		333.3
	3	1.03-1.09	3.98	0.36			0.63	1.5
Fi 88	1	0.27-0.34	0.38	0.22	39			24.4
	2	0.25-0.30	0.44	0.09	39			24.4
	3	0.26-0.31	0.29	0.20	34			21.2
	4	0.21-0.25	0.35	0.15	24.5			15.3
	5	0.24-0.28	0.28	0.11	28			17.5
	6	0.31-0.38	0.27	0.17	28			17.5
	7	0.24-0.29	0.26	0.10	32			20.0
	8	0.18-0.21	0.23	0.24	31			19.4
	9	0.19-0.23	0.27	0.13	25			15.6

Table II (cont.)

Notation	Porosity % Method 1 P1	Porosity % Method 2 P2	α-value % P3	Effective diffusivity, 10^{-14} m^2/s Iodide	Uranine	Cr-EDTA	Formation factor 10^{-5}
Fi 89 1	0.54-0.64	0.43	0.37	26			16.2
2	0.54-0.60	0.50	0.32	32			20.0
3	0.50-0.54	0.39	0.26	44			27.5
4	0.40-0.43	0.43	0.38	25			15.6
5	0.35-0.37	0.28	0.34	27			16.9
6	0.32-0.34	0.24	0.34	22.6			14.1
7	0.28-0.31	0.19	0.36	22			13.8
8	0.25-0.28	0.30	0.28	24			15.0
9	0.27-0.30	0.21	0.41	24.8			15.5
10	0.26-0.27	0.19	0.37	25			15.6
11	0.26-0.27	0.27	0.47	26.5			16.6
12	0.27-0.28	0.26	0.41	25.3			15.8
13	0.28-0.30	0.21	0.37	24.7			15.4
14	0.28-0.29	0.23	0.32	24.4			15.2
15	0.38-0.40	0.24	0.34	23.5			14.7
16	0.33-0.35	0.25	0.37	24.8			15.5
17	0.34-0.37	0.26	0.65	44			27.5

* 1 mol/l iodide solution and distilled water

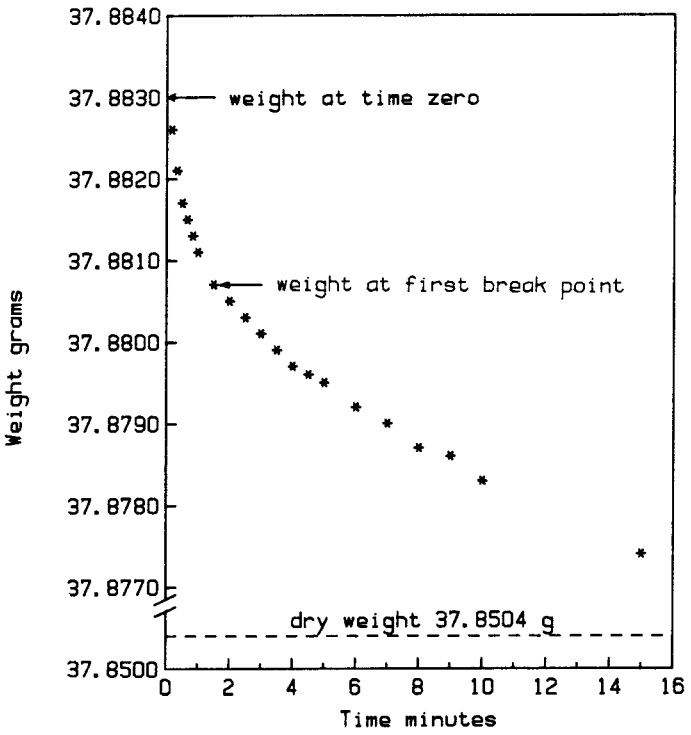

Figure 1: Weight of a water saturated granite sample versus time.

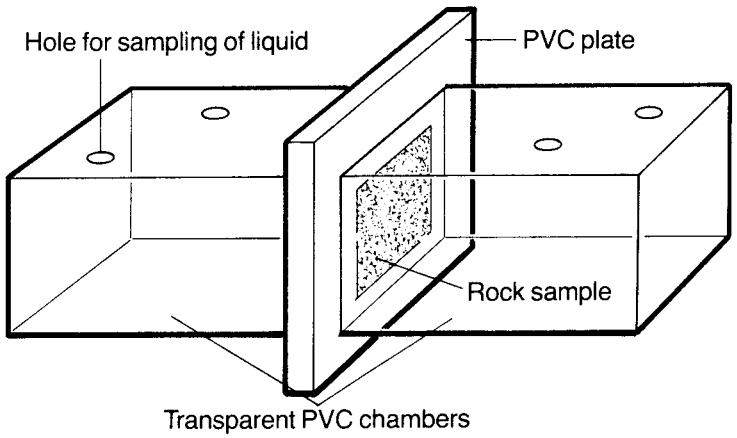

Figure 2: The diffusion cell.

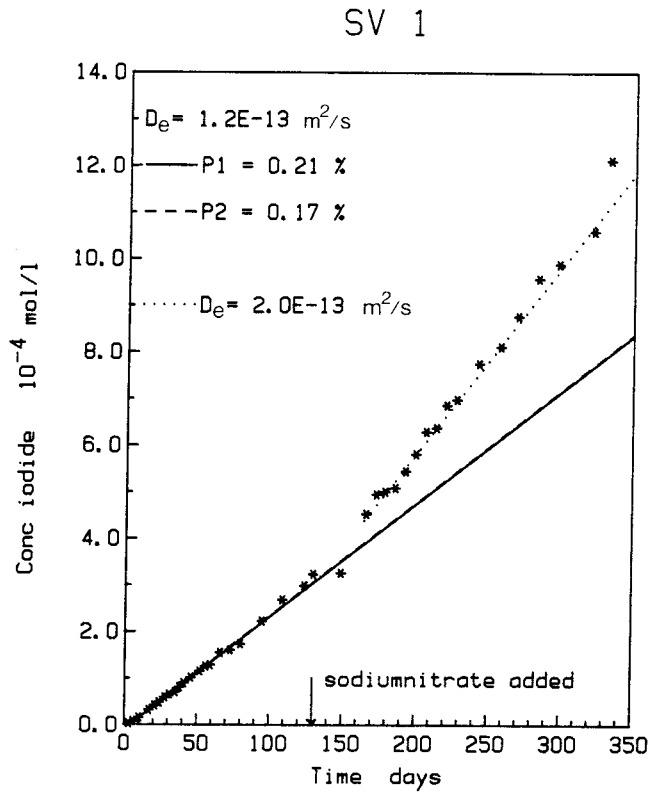

Figure 3: Concentration versus time for iodide diffusion through migmatite from Studsvik.

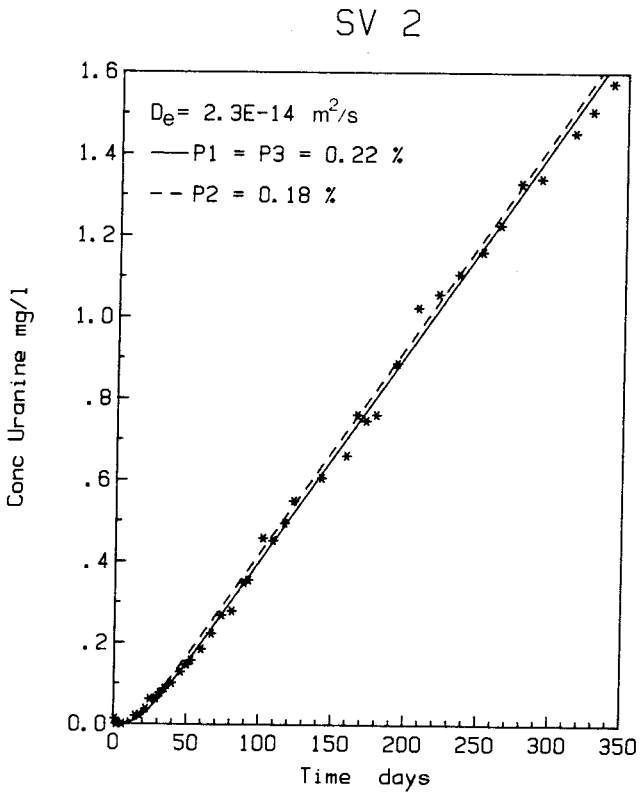

Figure 4: Concentration versus time for Uranine diffusion through migmatite from Studsvik.

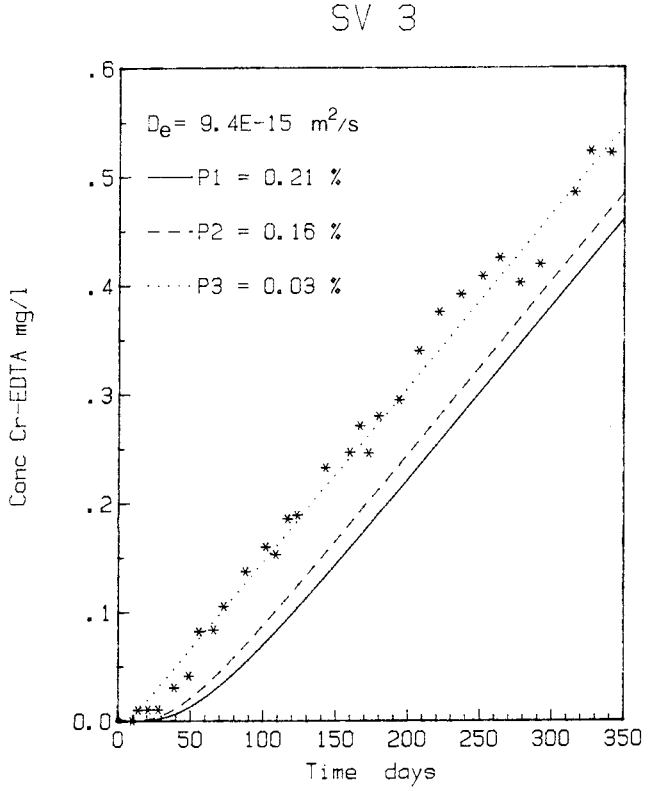

Figure 5: Concentration versus time for Cr-EDTA diffusion through migmatite from Studsvik.

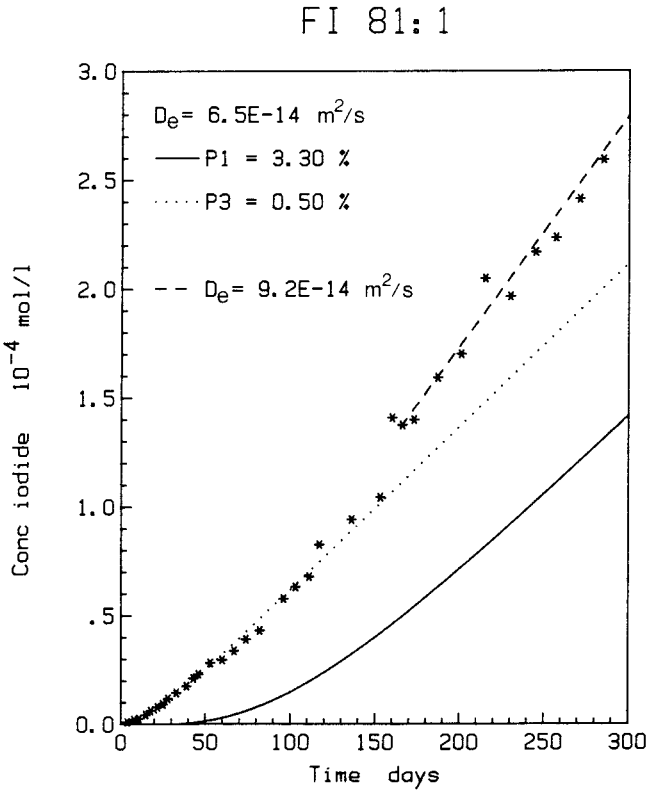

Figure 6: Concentration versus time for iodide diffusion through granite+fissure coating material from Finnsjön, Fi 81.

FI 81:1

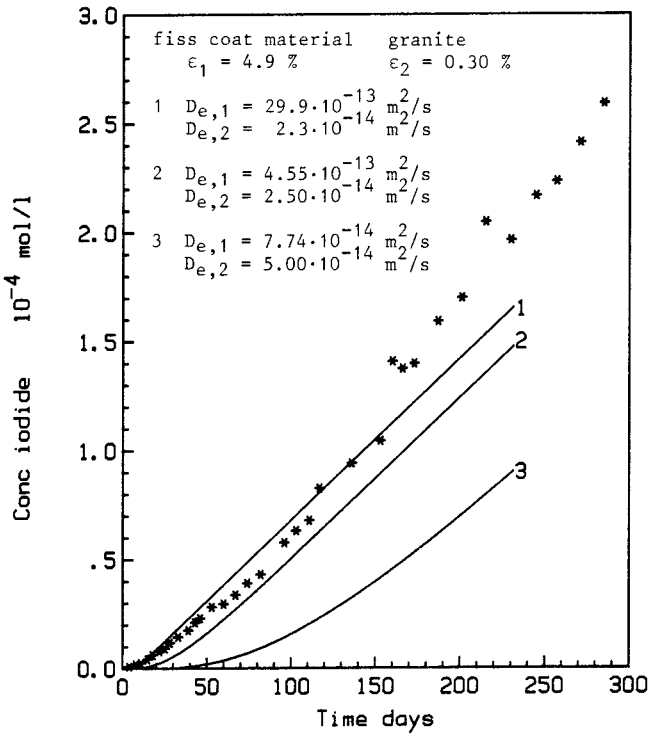

Figure 7: Experimental data for iodide diffusion through Fi 81 and theoretical curves simulating diffusion through two layers in serie with different diffusivities and porosities in each layer.

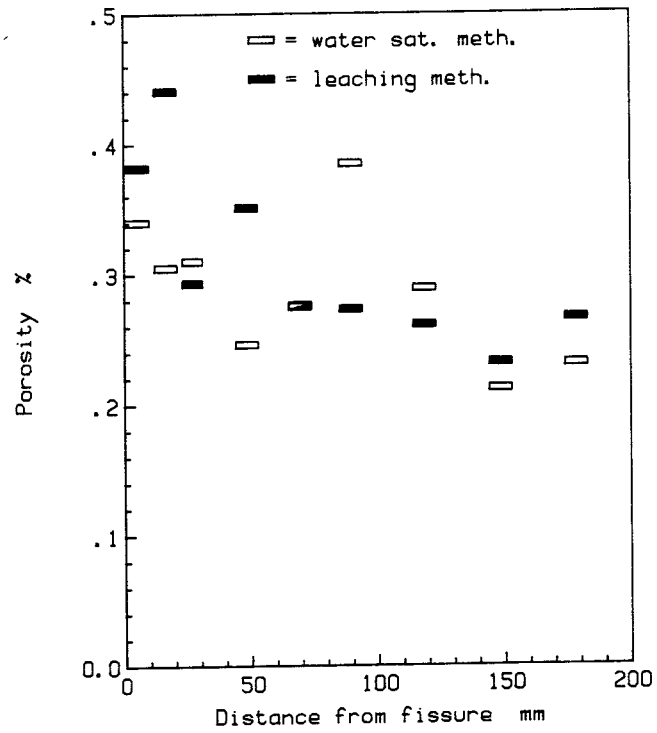

Figure 8: Porosity of samples from Finnsjön, Fi 88, versus distance from a fissure surface.

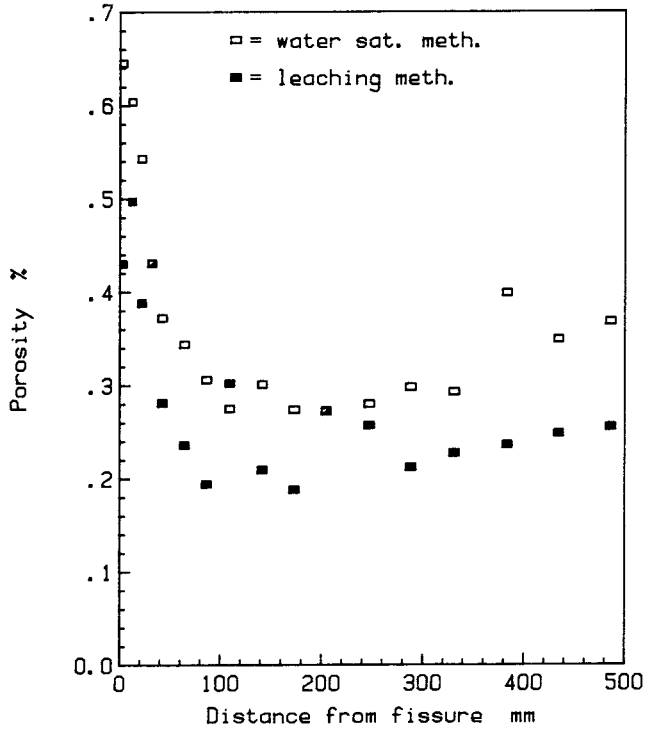

Figure 9: Porosity of samples from Finnsjön, Fi 89, versus distance from a fissure surface.

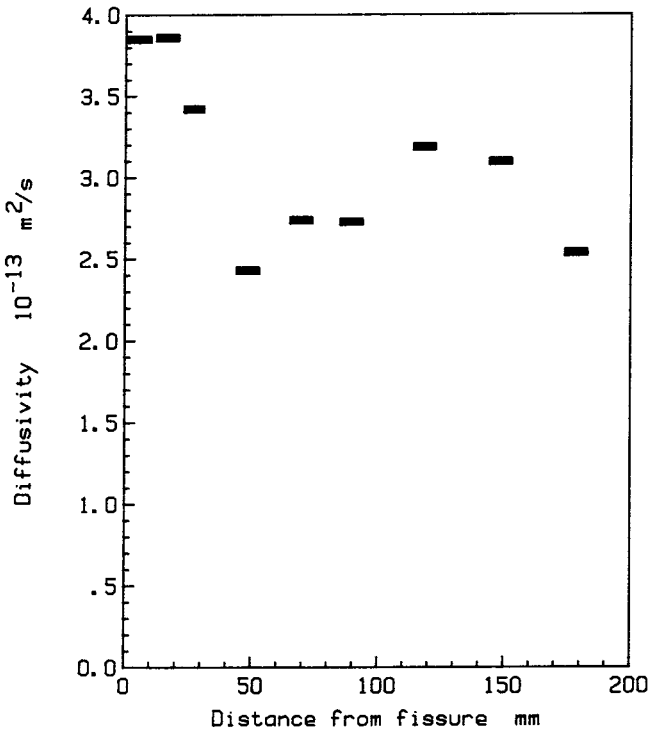

Figure 10: Effective diffusivity in samples from Finnsjön, Fi 88, versus distance from a fissure surface.

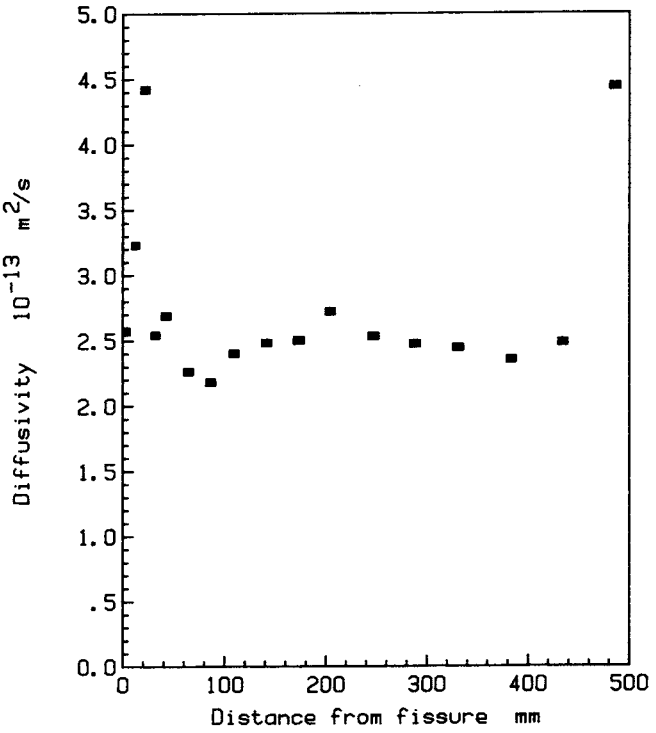

Figure 11: Effective diffusivity in samples from Finnsjön, Fi 89, versus distance from a fissure surface.

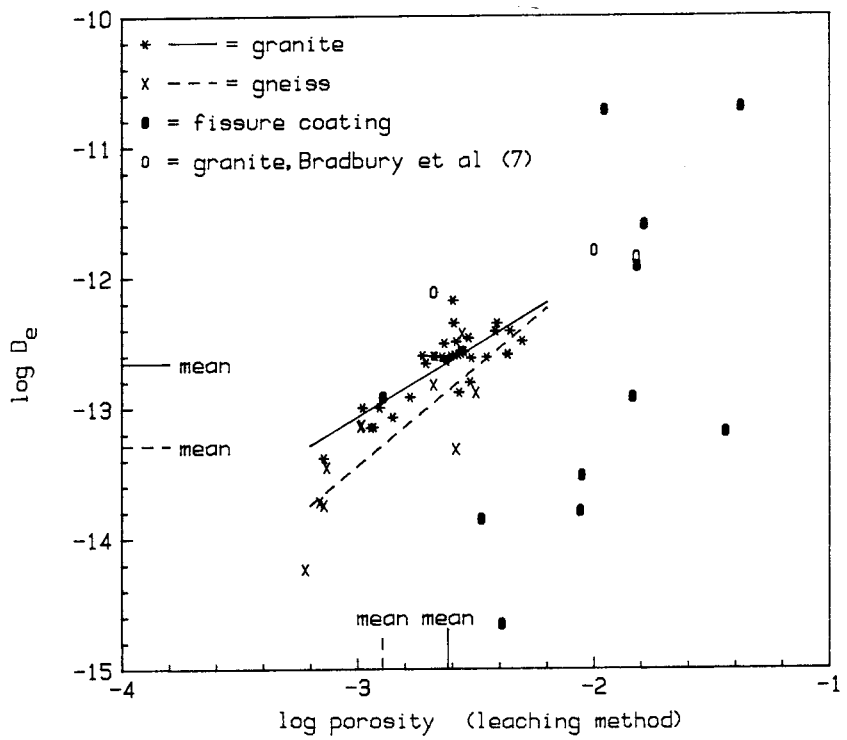

Figure 12: The logarithmic value of the effective diffusivity of iodide in the rock materials versus the logarithmic value of the porosity from the leaching method (P2).

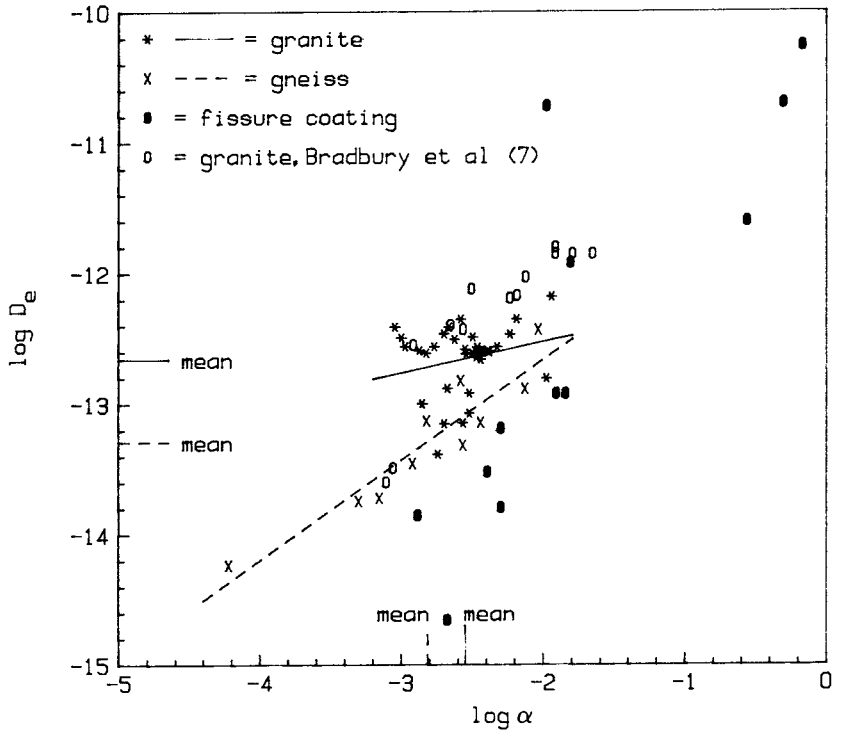

Figure 13: The logarithmic value of the effective diffusivity of iodide in the rock materials versus the logarithmic value of α from eq. 7.

Appendix to the paper "Porosities of and diffusivities of some non-sorbing species in crystalline rocks".

Kristina Skagius, Ivars Neretnieks

1985-02-07

Concentraiton versus time plots, experimental data and theoretical curves.

P1 = Porosity measured by the water saturation method
P2 = Porosity measured by the leaching method
P3 = α-value from eq. 7
D_e = effective diffusivity

F 1

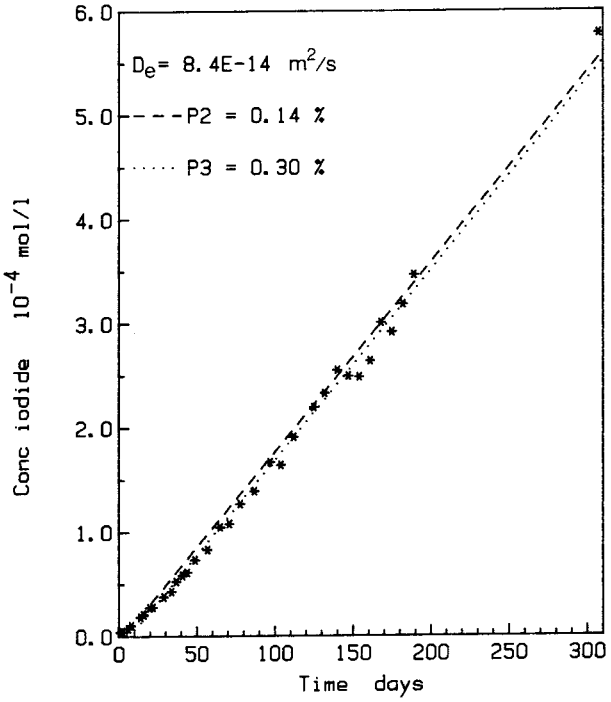
De= 8.4E-14 m²/s
P2 = 0.14 %
P3 = 0.30 %
Conc iodide 10⁻⁴ mol/l
Time days

F 2

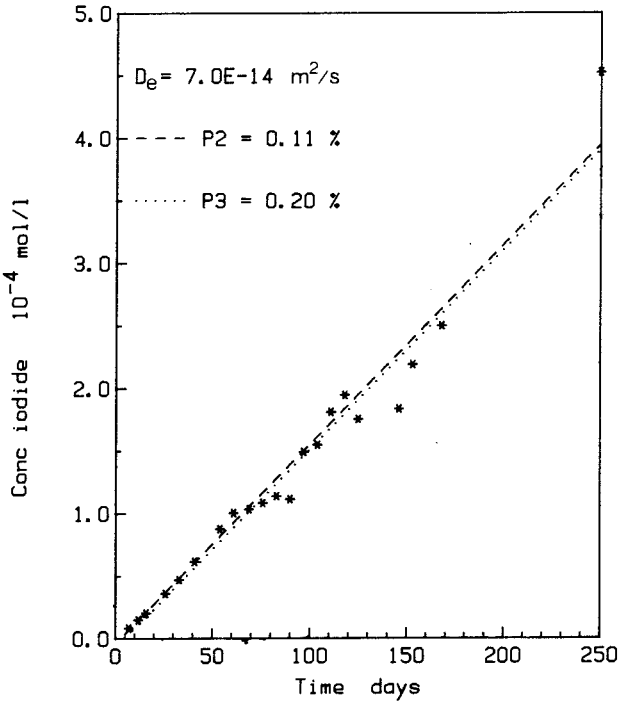
De= 7.0E-14 m²/s
P2 = 0.11 %
P3 = 0.20 %
Conc iodide 10⁻⁴ mol/l
Time days

F 3

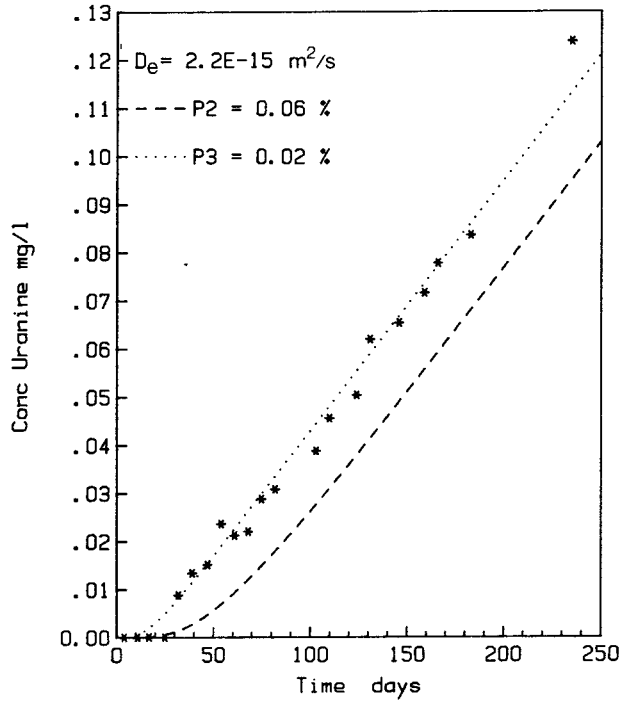
De= 2.2E-15 m²/s
P2 = 0.06 %
P3 = 0.02 %
Conc Uranine mg/l
Time days

F 5

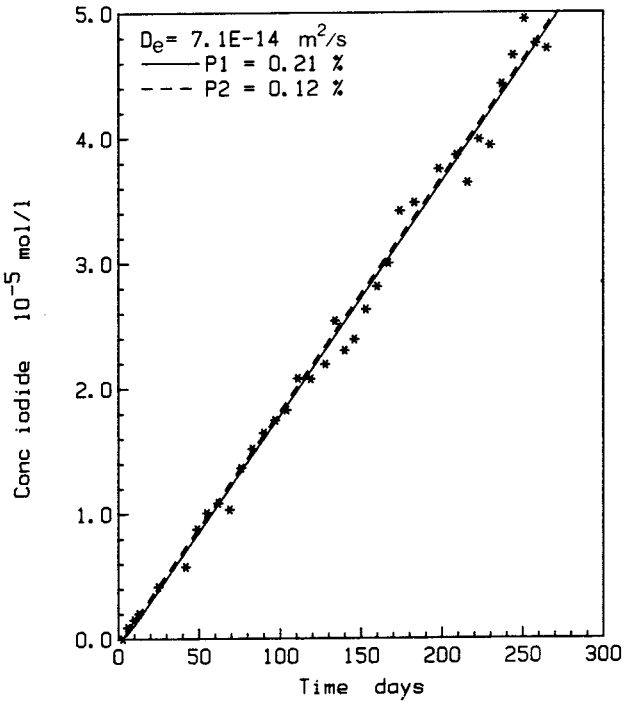
De= 7.1E-14 m²/s
P1 = 0.21 %
P2 = 0.12 %
Conc iodide 10⁻⁵ mol/l
Time days

F 6

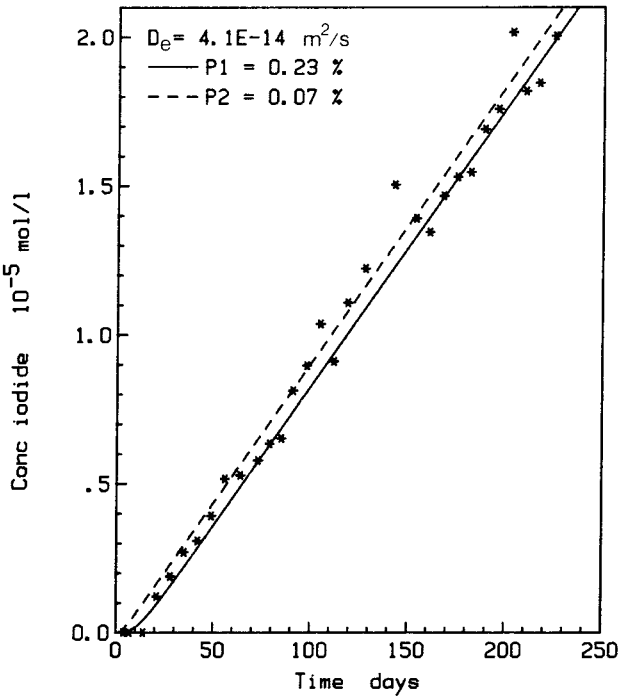
De= 4.1E-14 m²/s
P1 = 0.23 %
P2 = 0.07 %
Conc iodide 10⁻⁵ mol/l
Time days

F 7

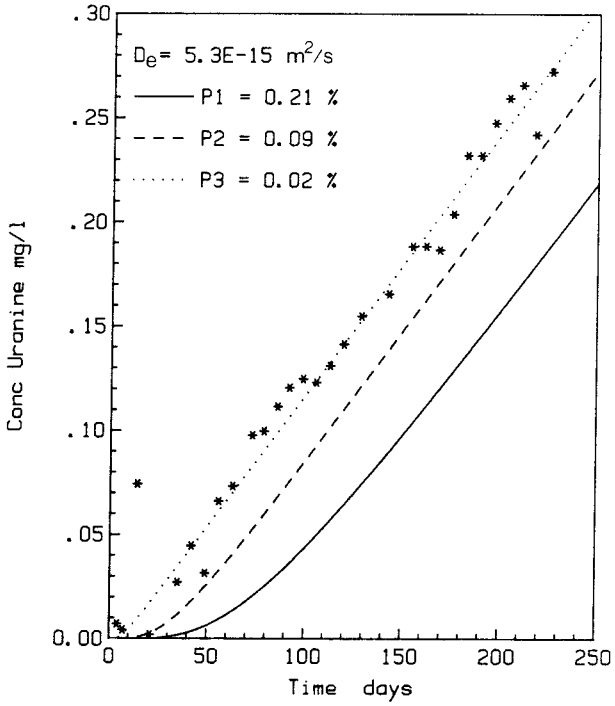
De= 5.3E-15 m²/s
P1 = 0.21 %
P2 = 0.09 %
P3 = 0.02 %
Conc Uranine mg/l
Time days

F 8

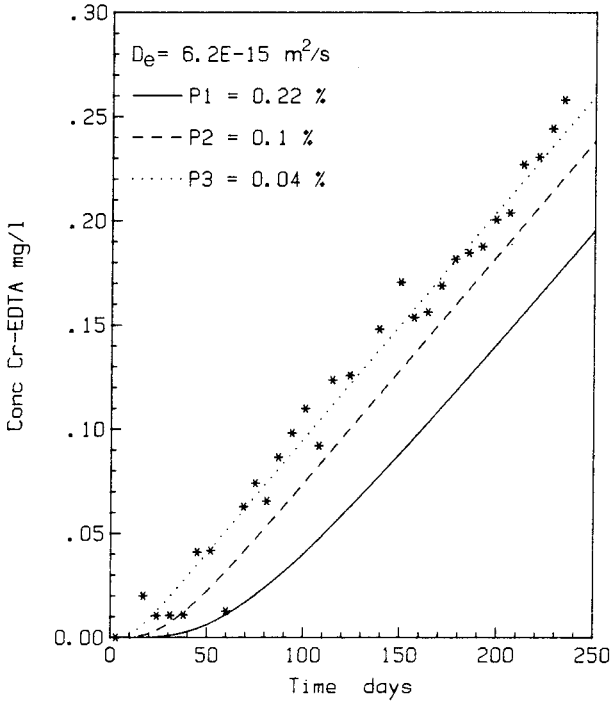
De= 6.2E-15 m²/s
P1 = 0.22 %
P2 = 0.1 %
P3 = 0.04 %
Conc Cr-EDTA mg/l
Time days

S 1

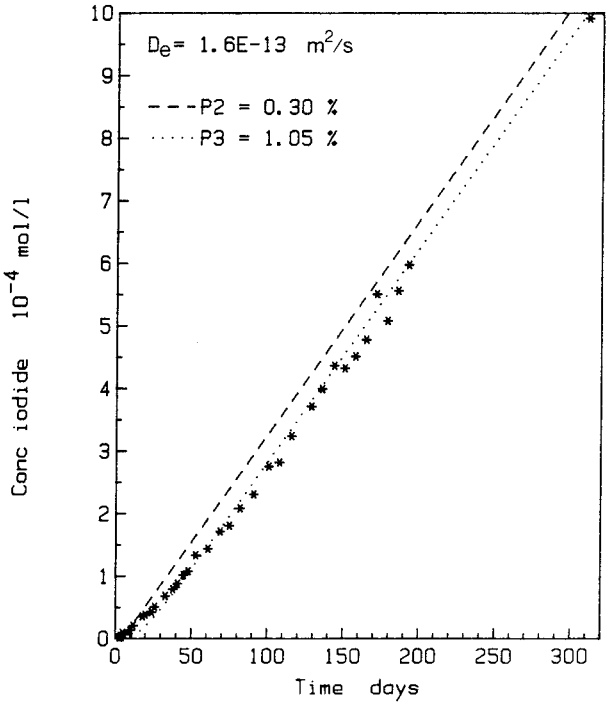
De= 1.6E-13 m²/s
P2 = 0.30 %
P3 = 1.05 %
Conc iodide 10⁻⁴ mol/l
Time days

S 2

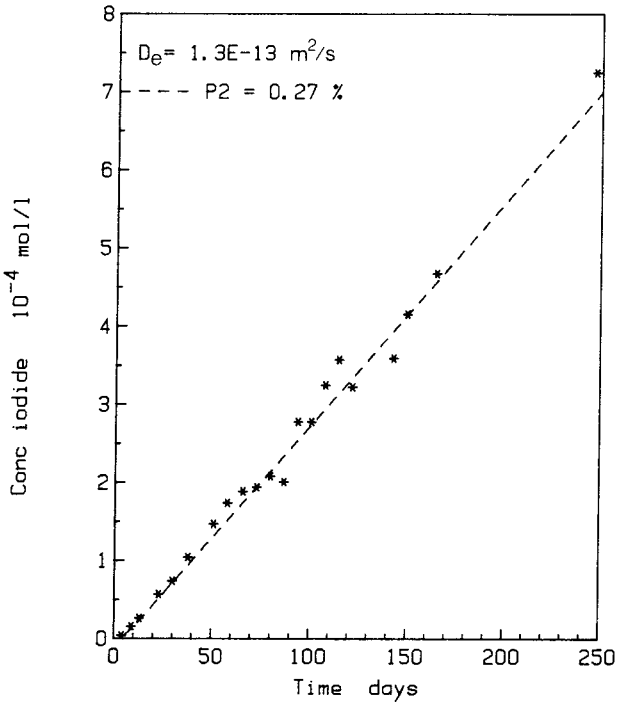

KG 1

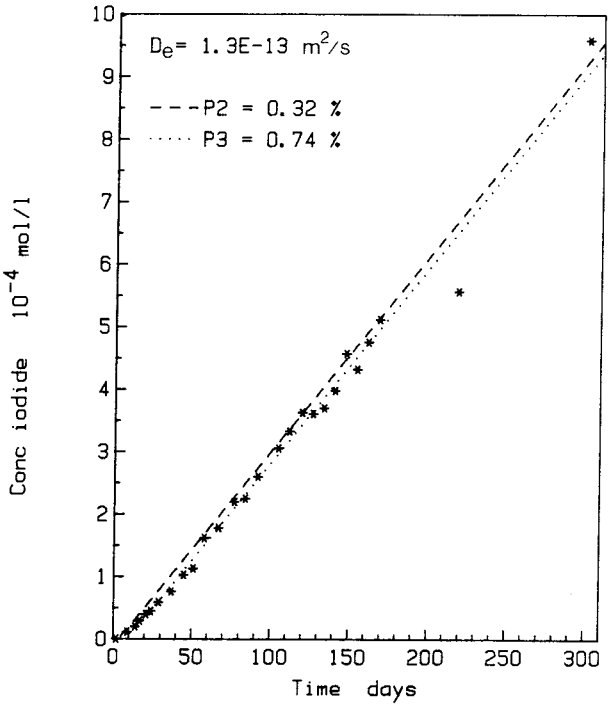

KG 2

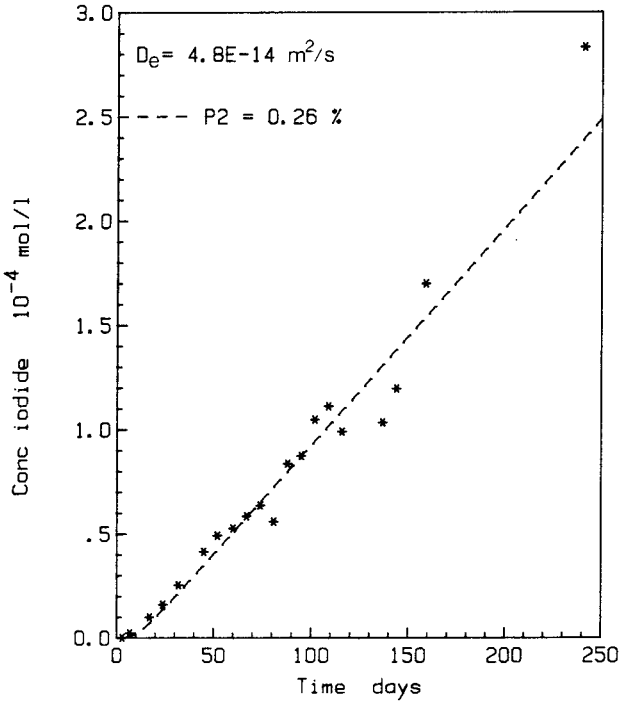

SV 1

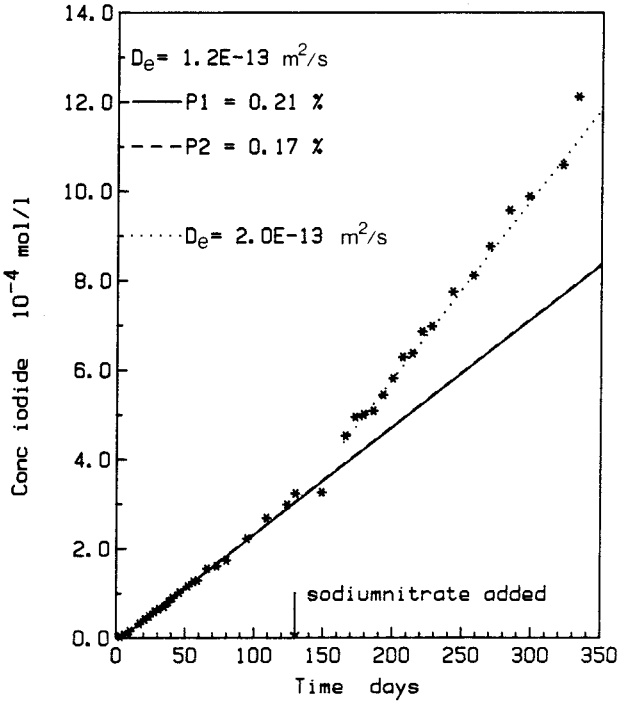

SV 2

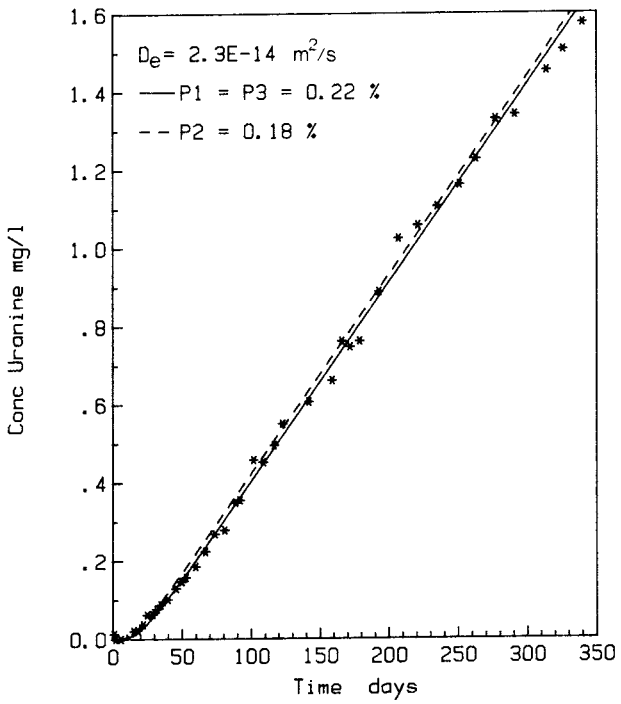
De= 2.3E-14 m²/s
P1 = P3 = 0.22 %
P2 = 0.18 %
Conc Uranine mg/l
Time days

SV 3

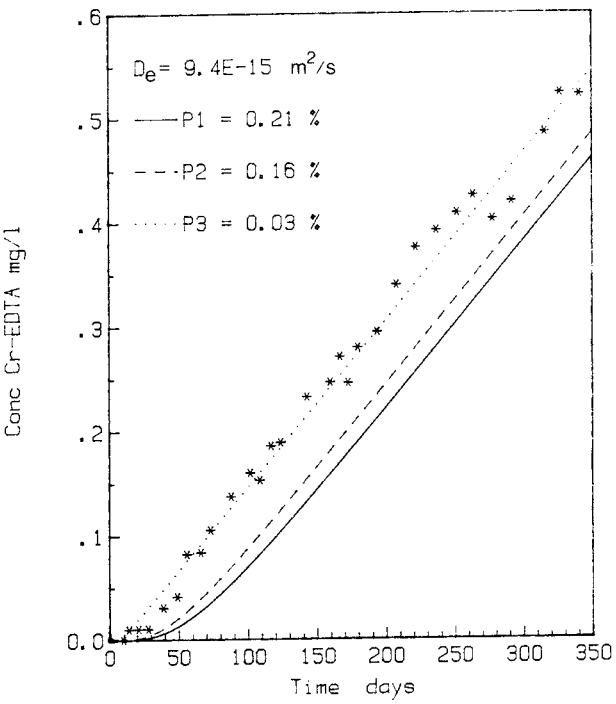
De= 9.4E-15 m²/s
P1 = 0.21 %
P2 = 0.16 %
P3 = 0.03 %
Conc Cr-EDTA mg/l
Time days

G 1

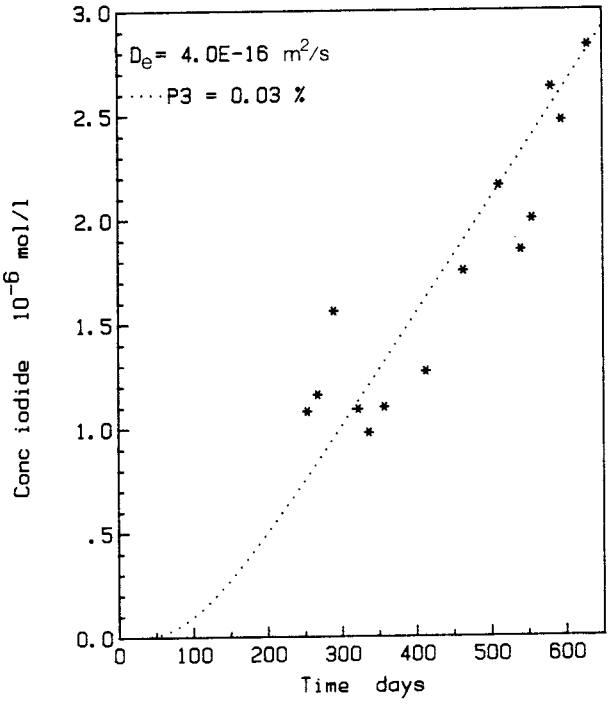
De= 4.0E-16 m²/s
P3 = 0.03 %
Conc iodide 10⁻⁶ mol/l
Time days

G 2

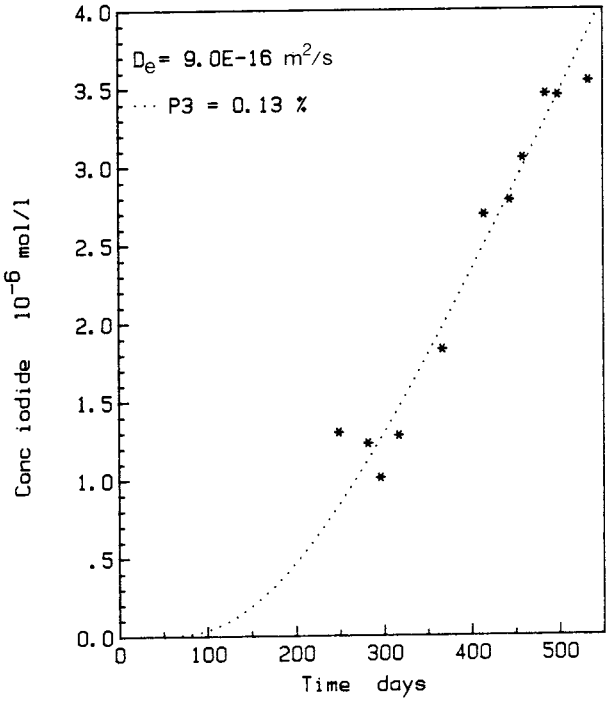
De= 9.0E-16 m²/s
P3 = 0.13 %
Conc iodide 10⁻⁶ mol/l
Time days

GAA1: 1

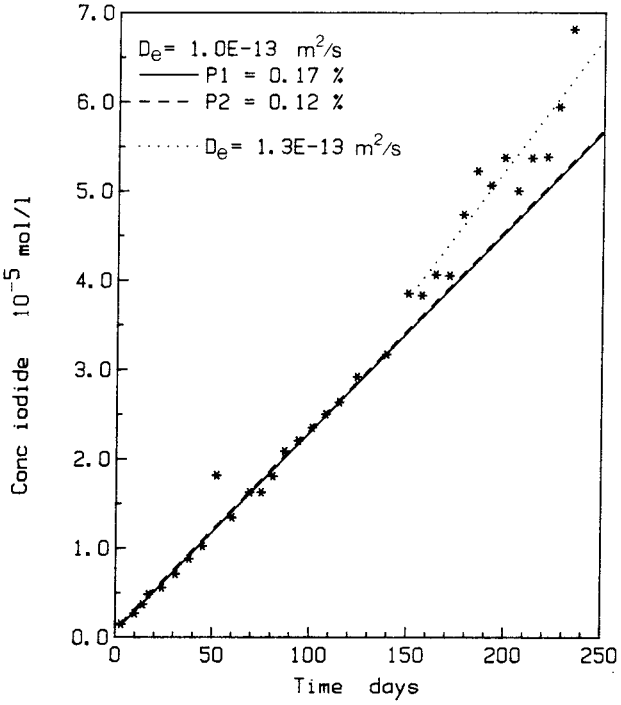

GAA1: 2

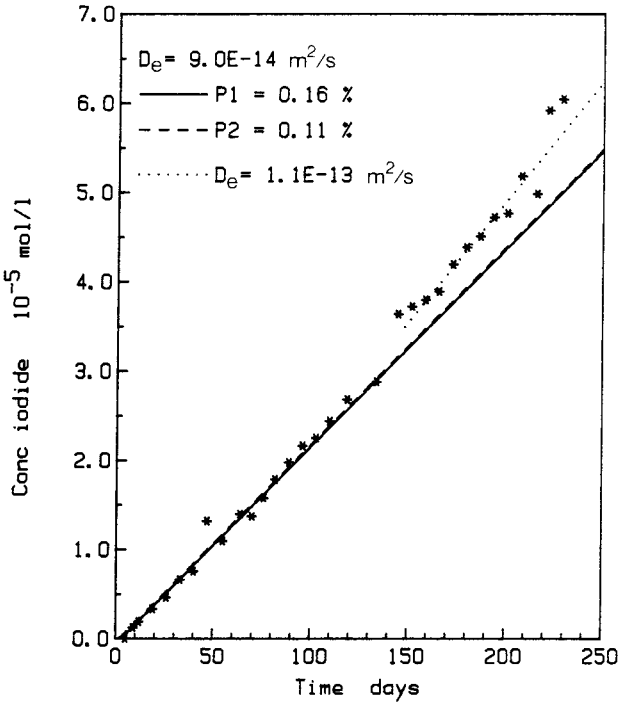

GAA 1: 3

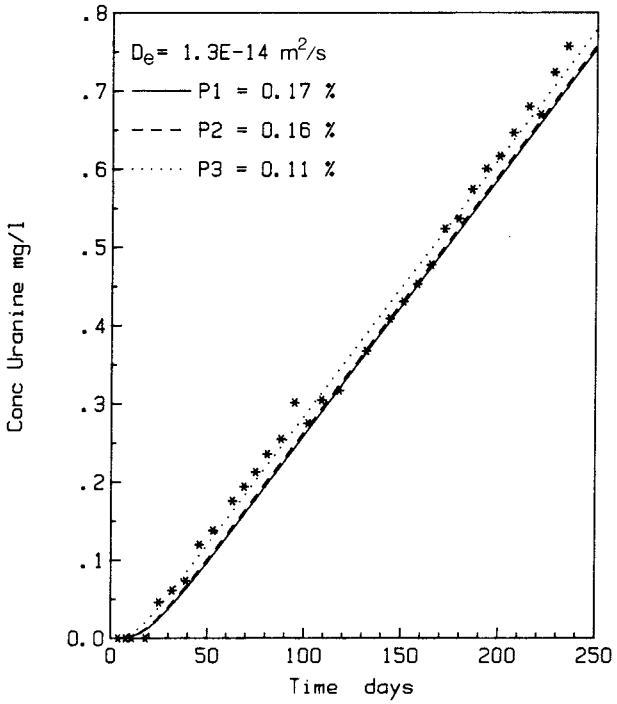

GAA 1: 4

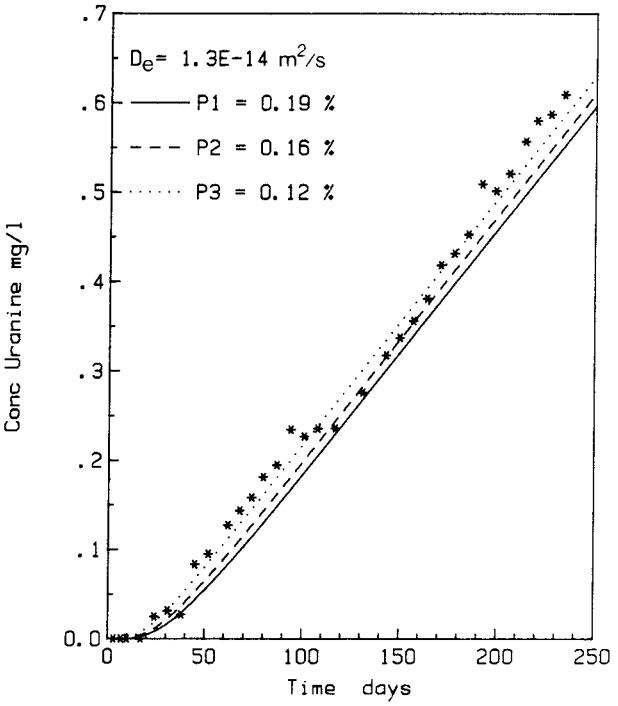

GAA 1:5

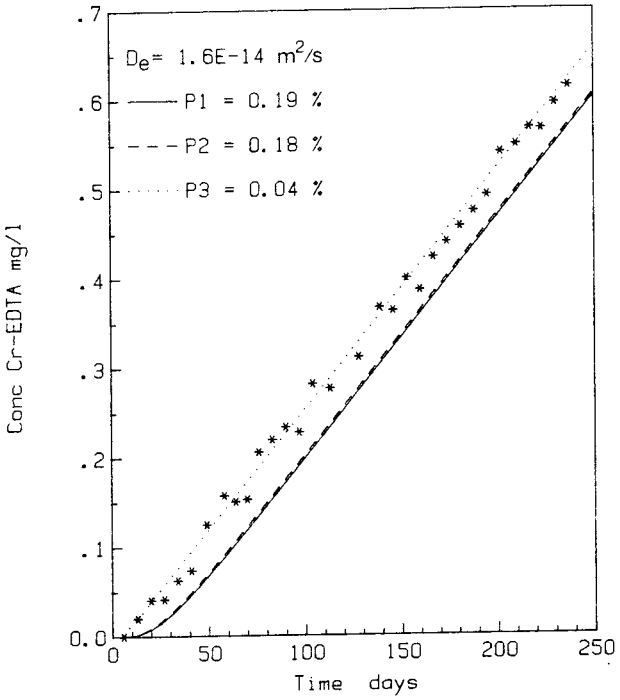

GAA 1:6

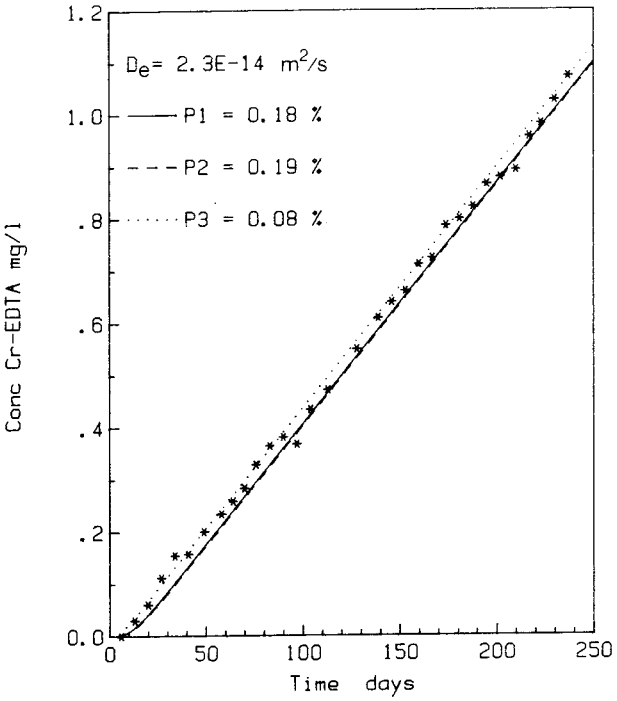

GAA 7:1

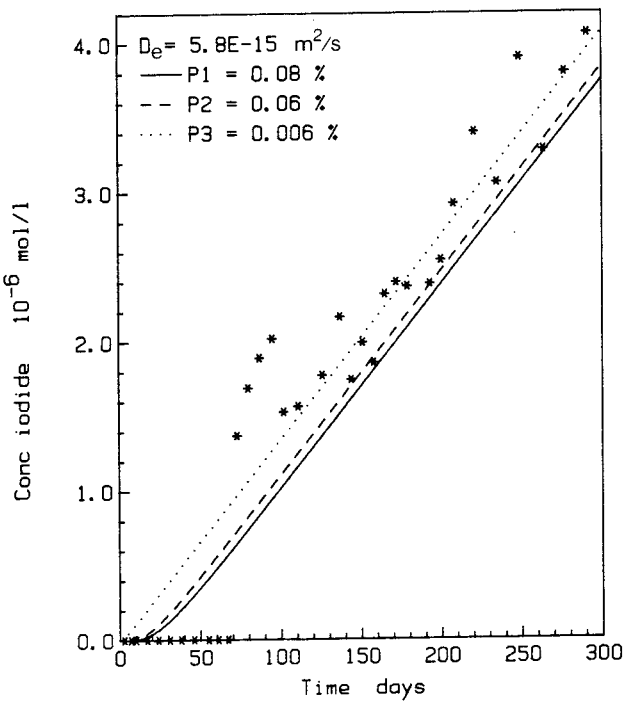

GAA 7:2

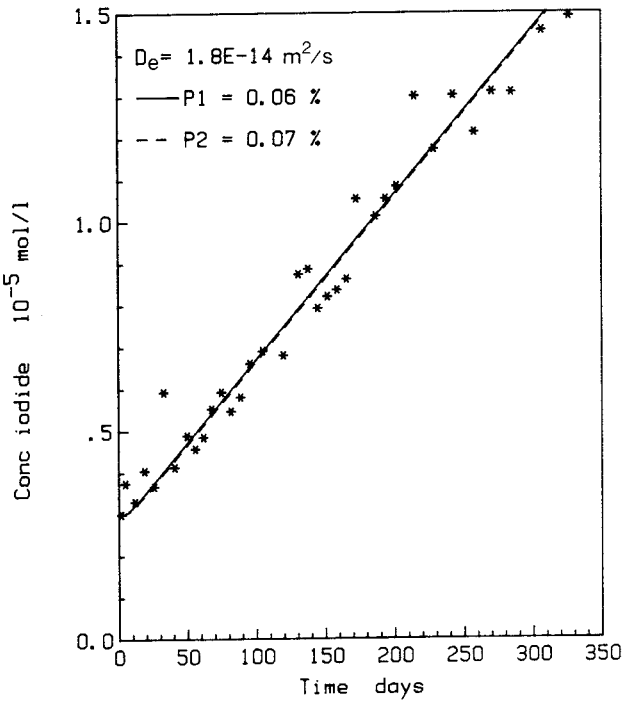

GAA 7: 3

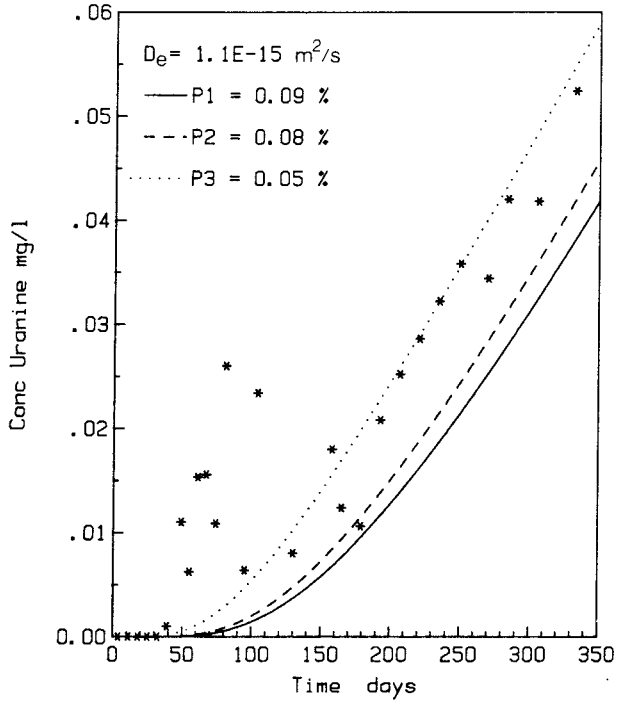

GAA 7: 4

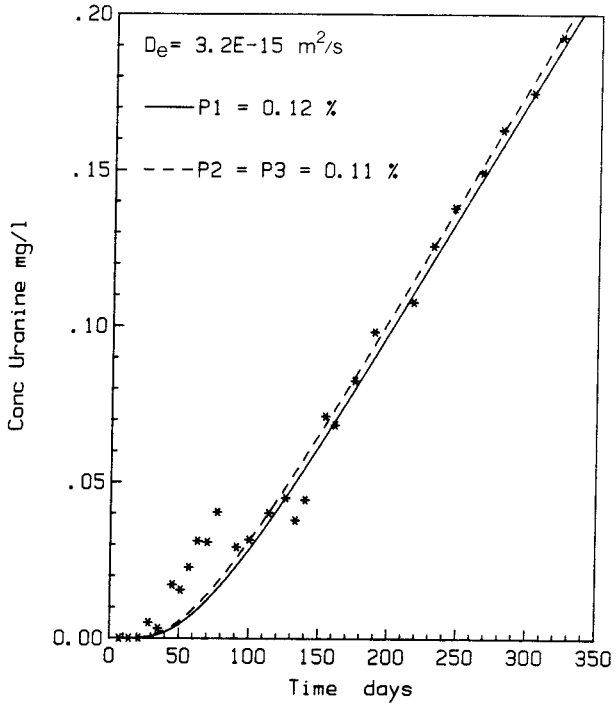

SB 1: 1

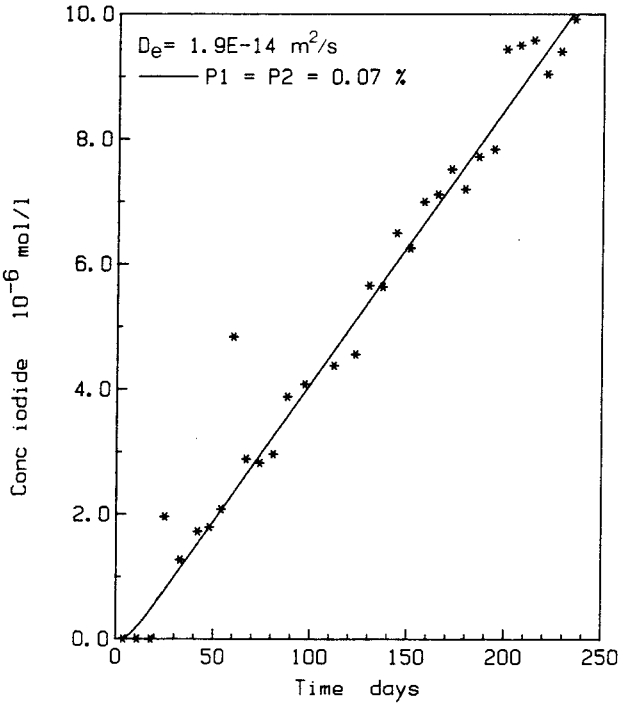

SB 1: 2

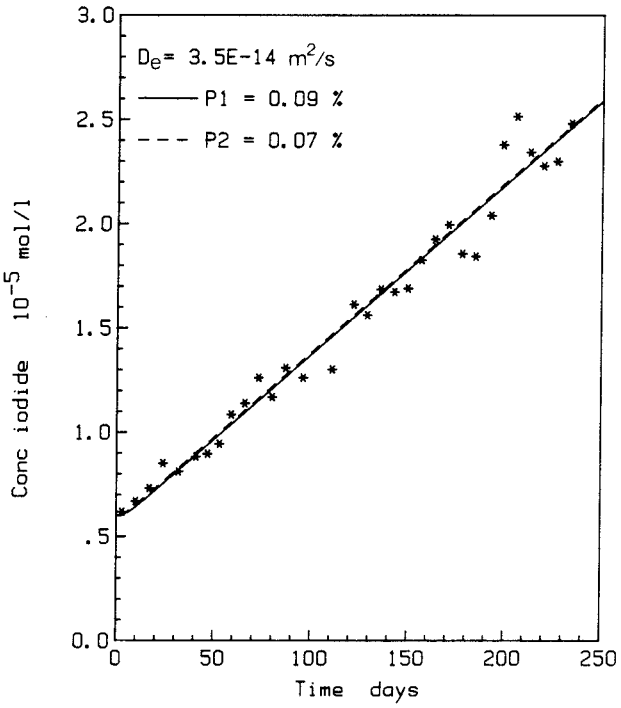

SB 1:3

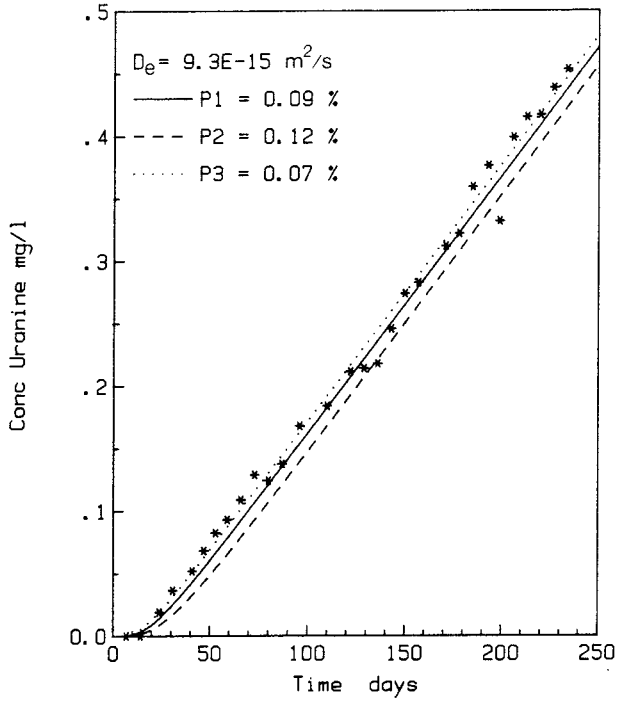

SB 1:4

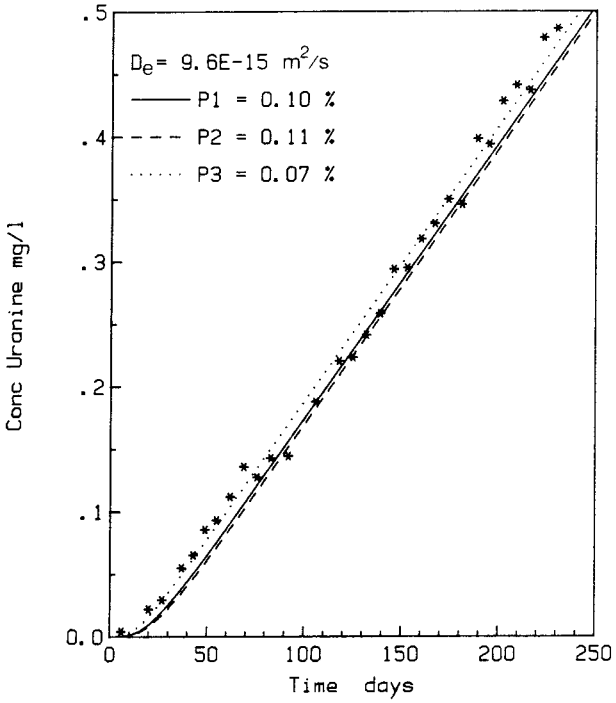

SB 1:5

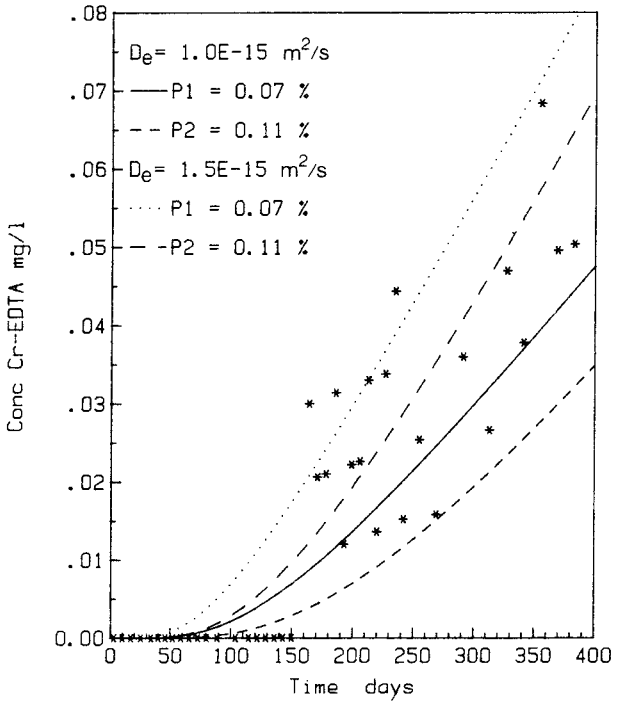

SB 1:6

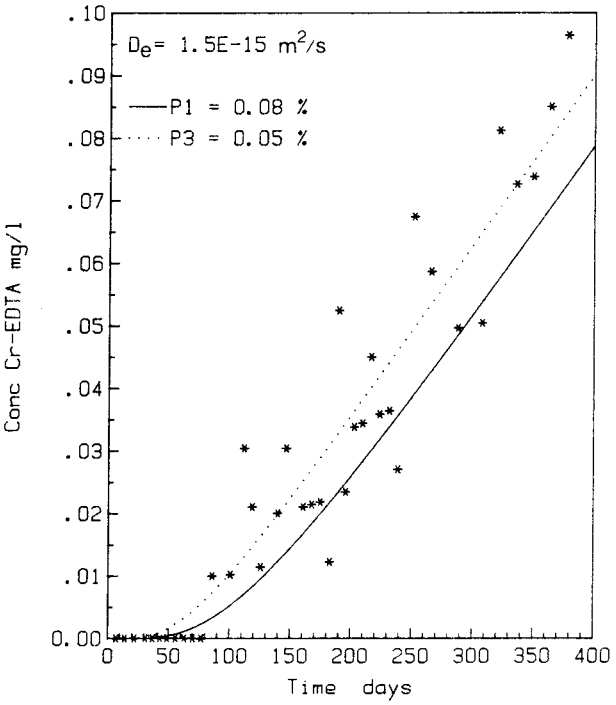

SB 7: 1

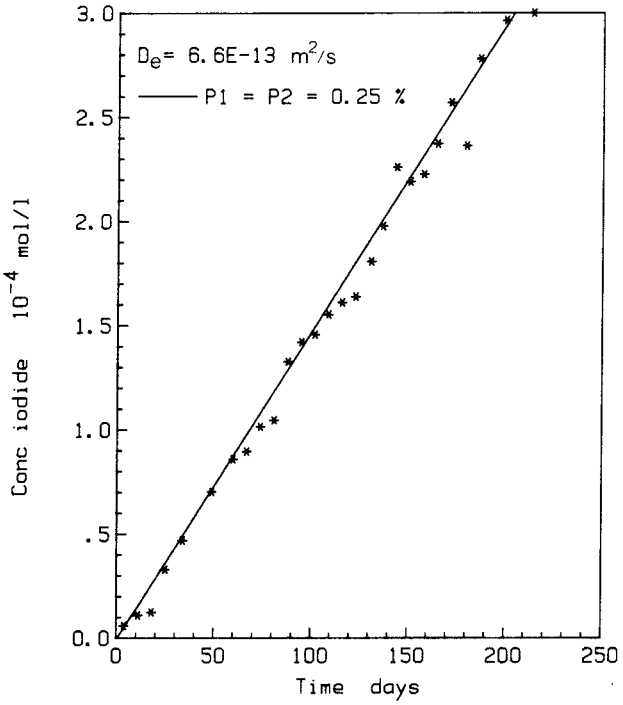

SB 7: 2

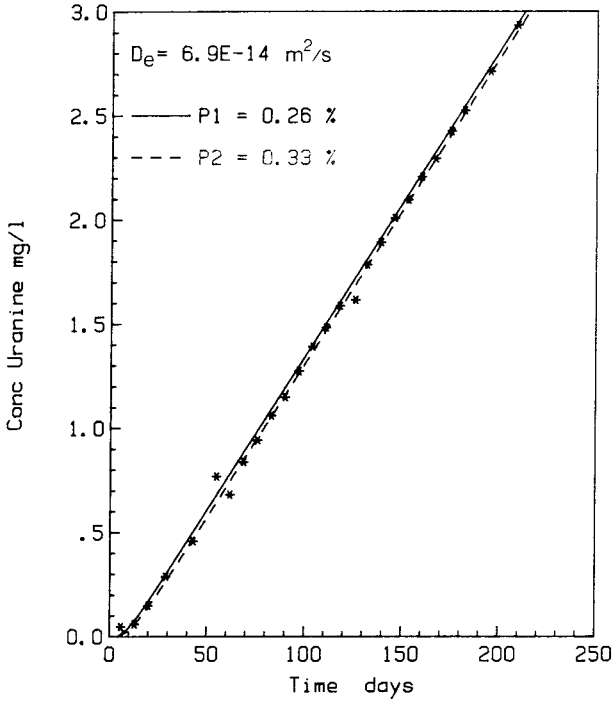

SB 7: 3

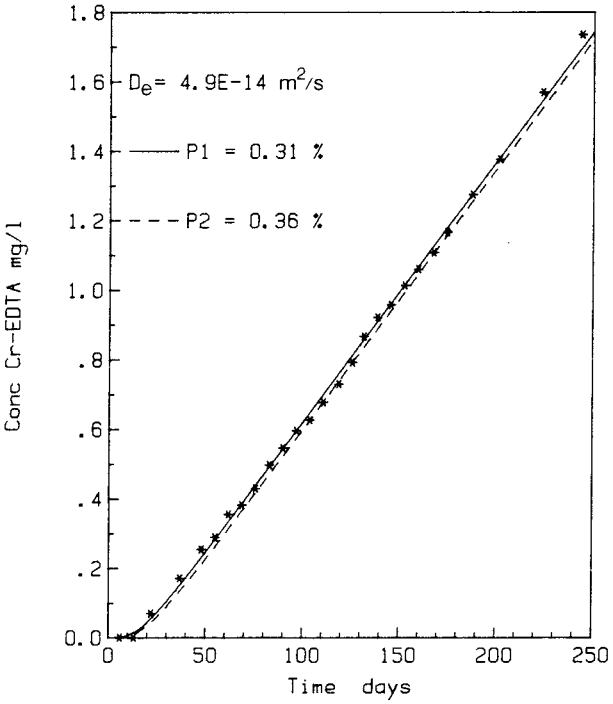

SB 7: 4

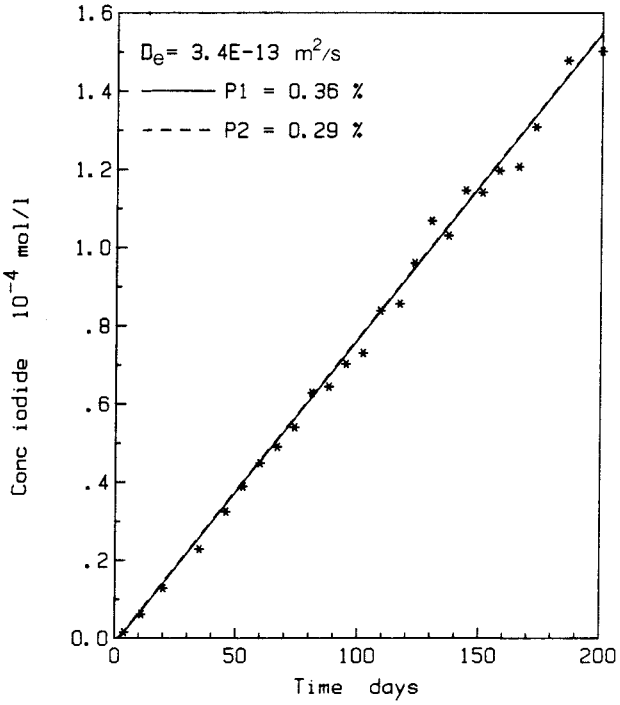

SB 7:5

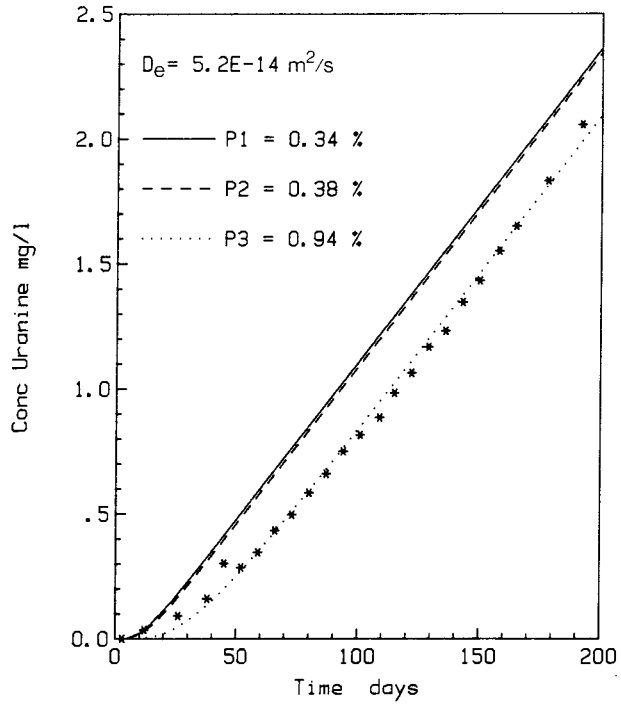

SB 7:6

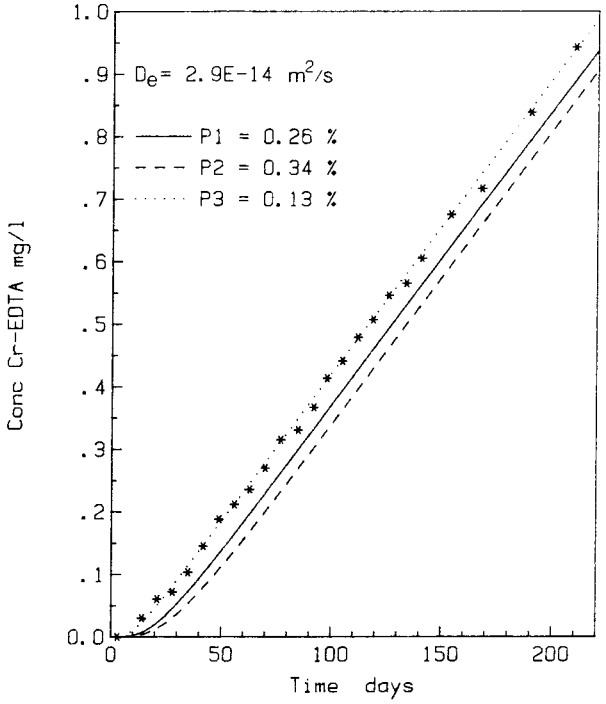

SB 7:7

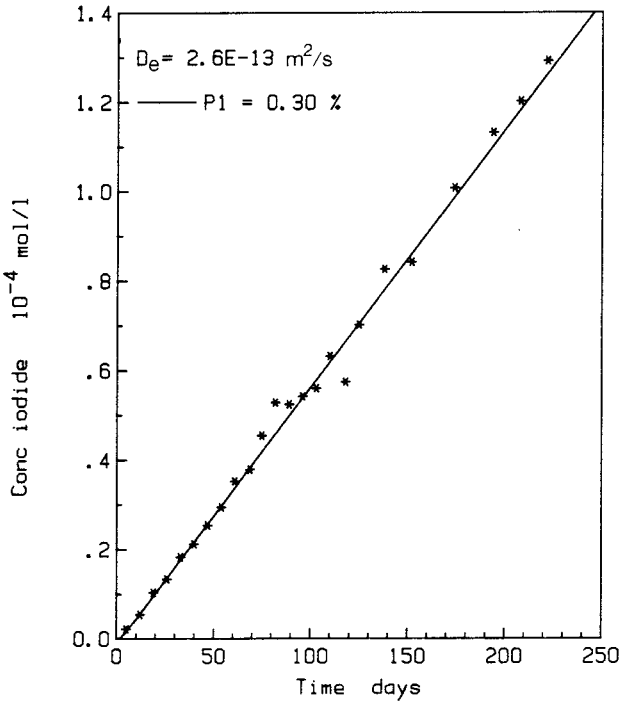

SB 21:1

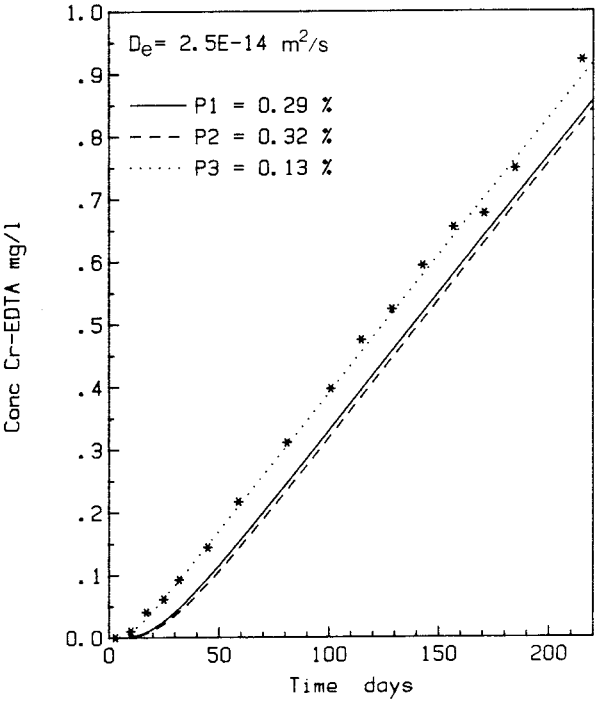

SB 21:2

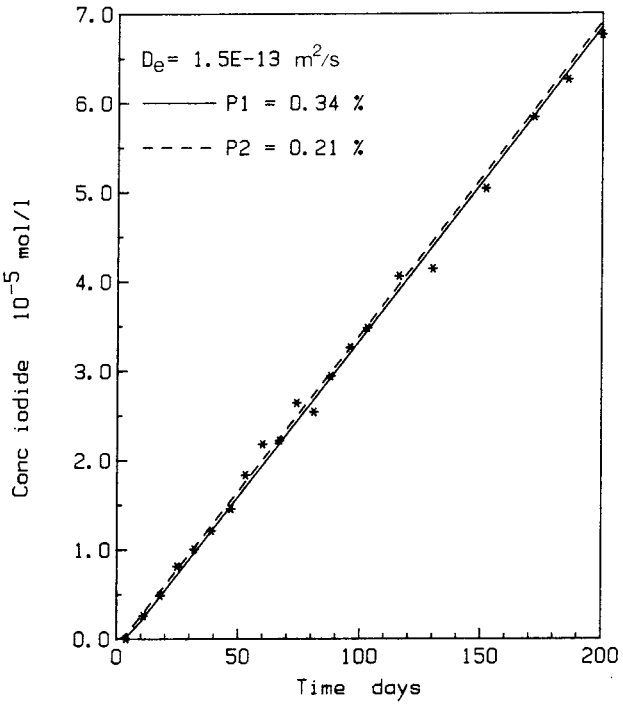

SB 21:3

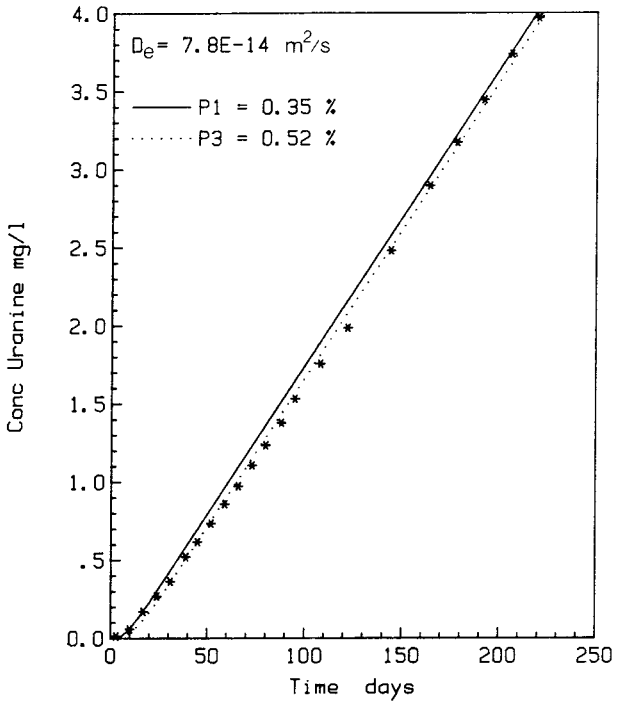

SB 21:4

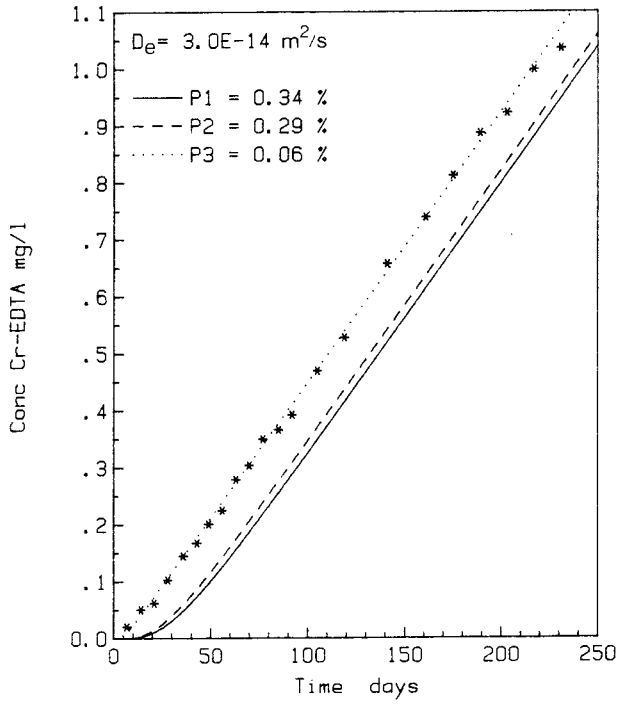

SB 21:5

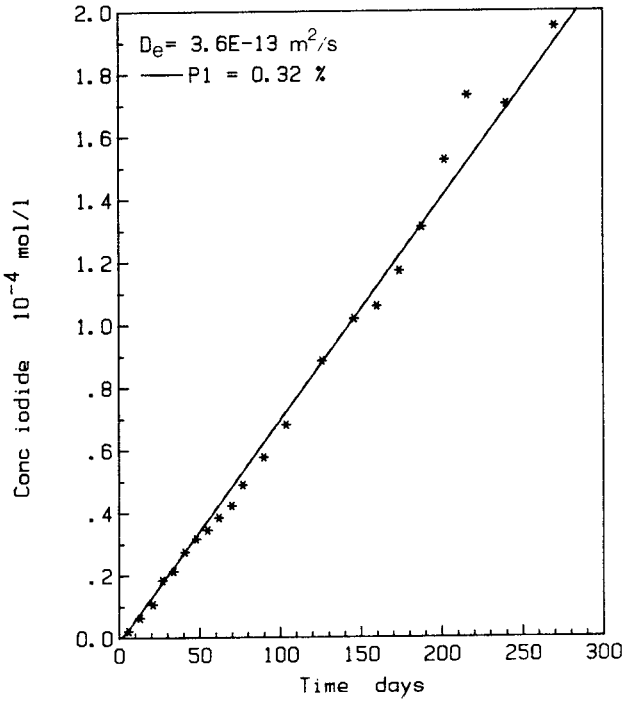

SB 21:6

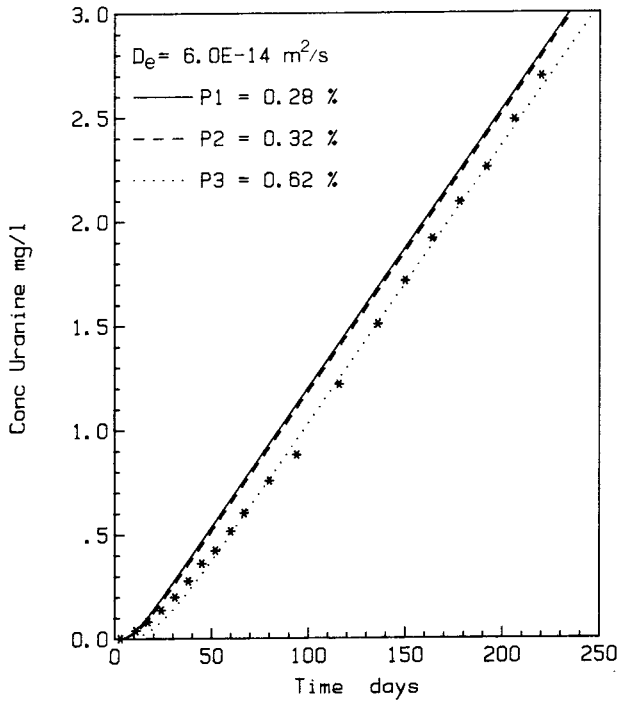

FJ 1:1

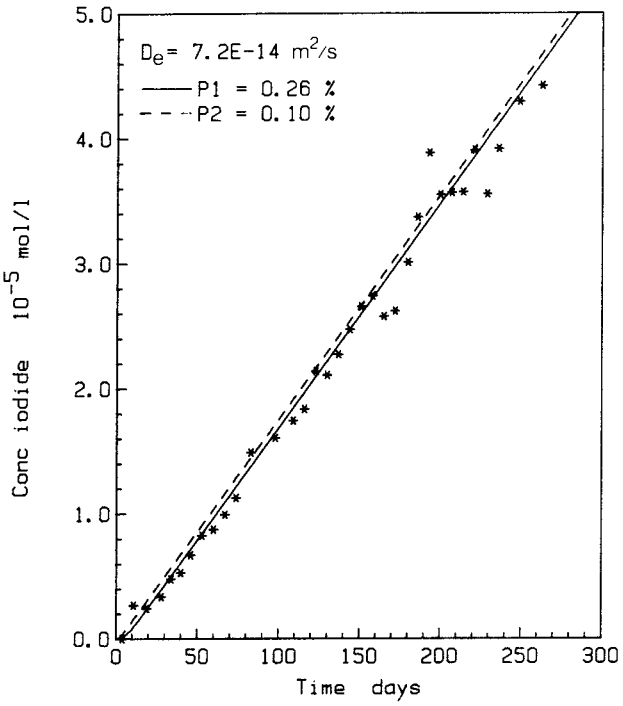

FJ 1:2

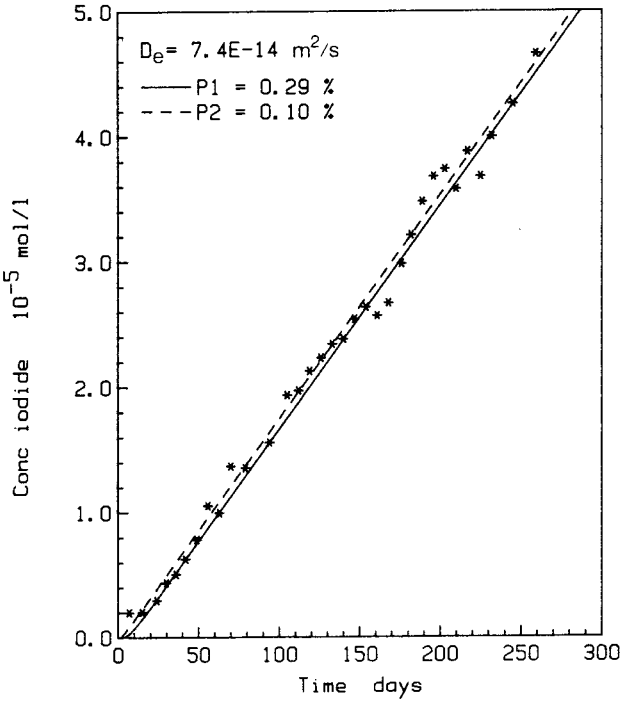

FJ 1:3

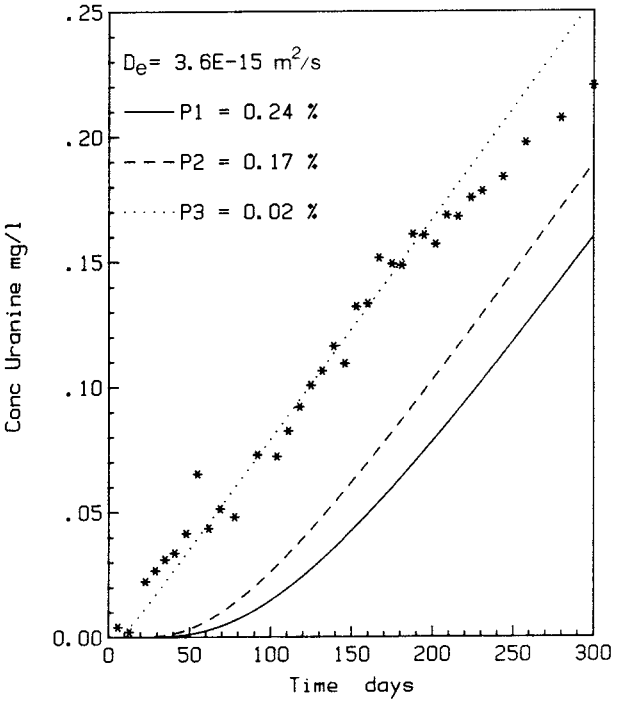

FJ 1:4

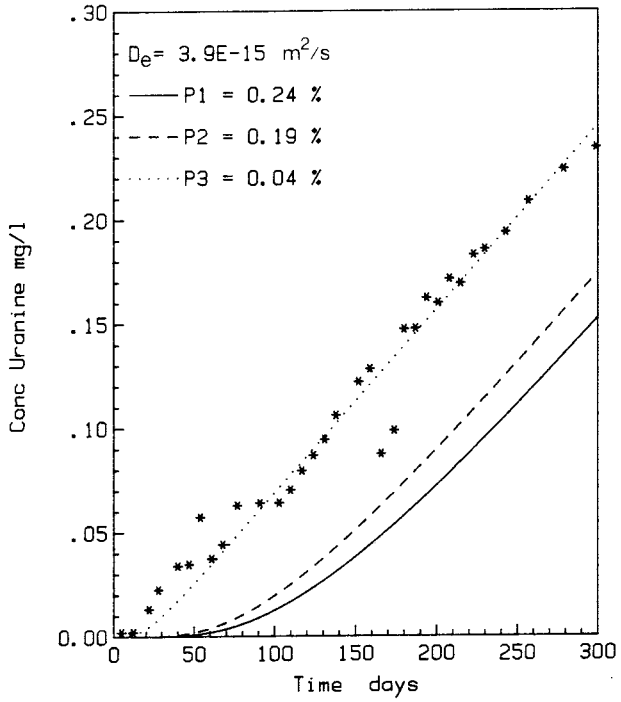

FJ 1:5

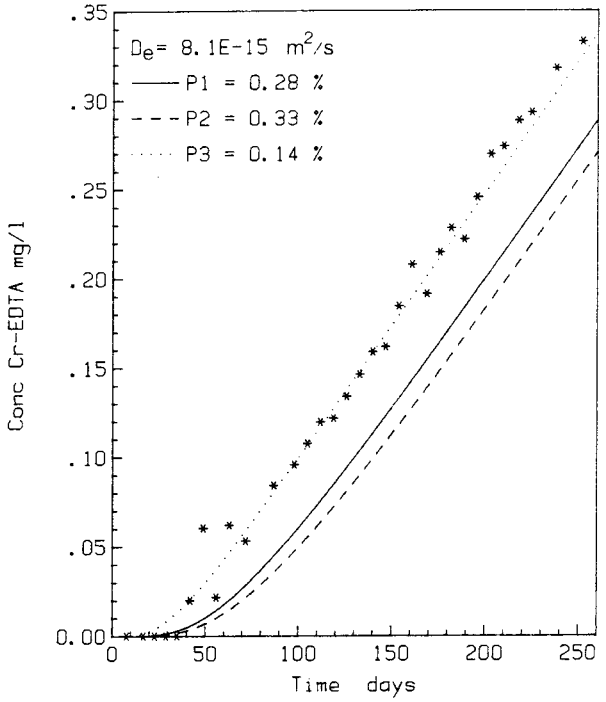

FJ 1:6

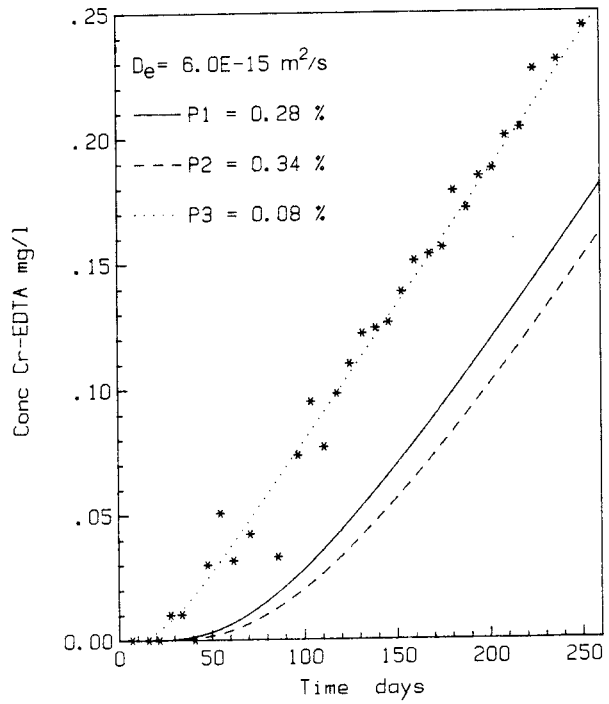

SP 1

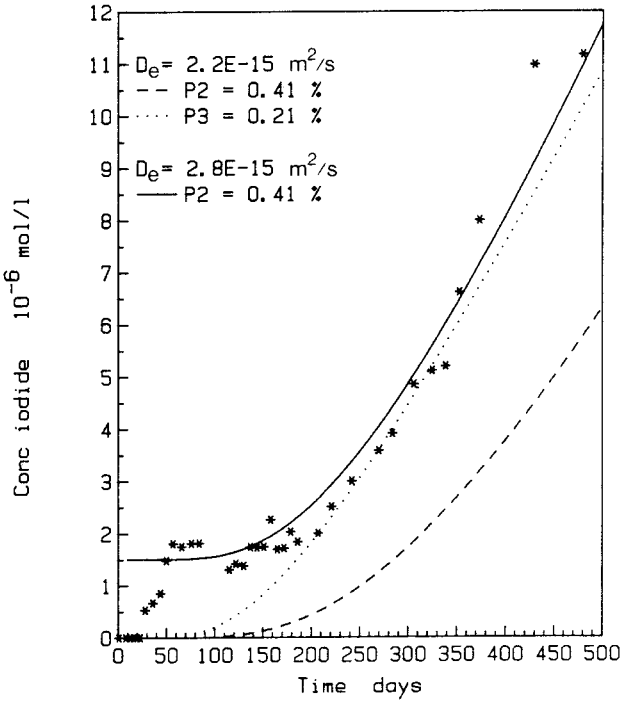

SP 2

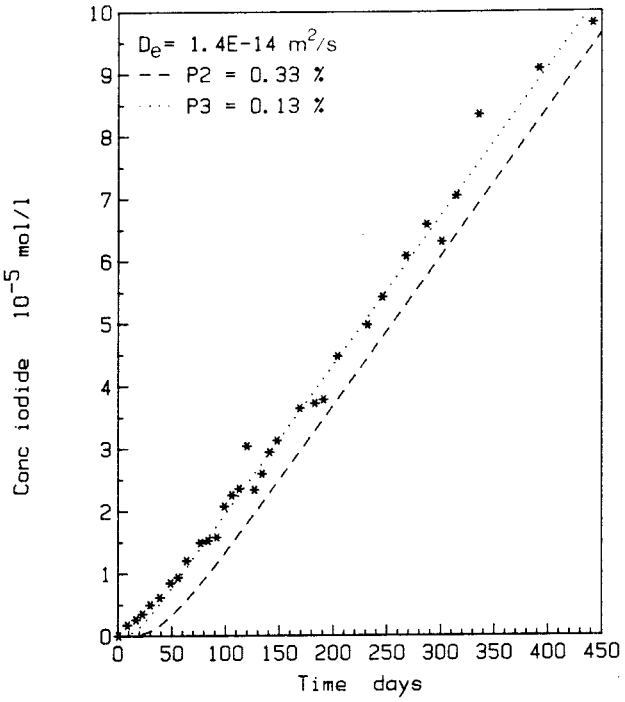

SS1

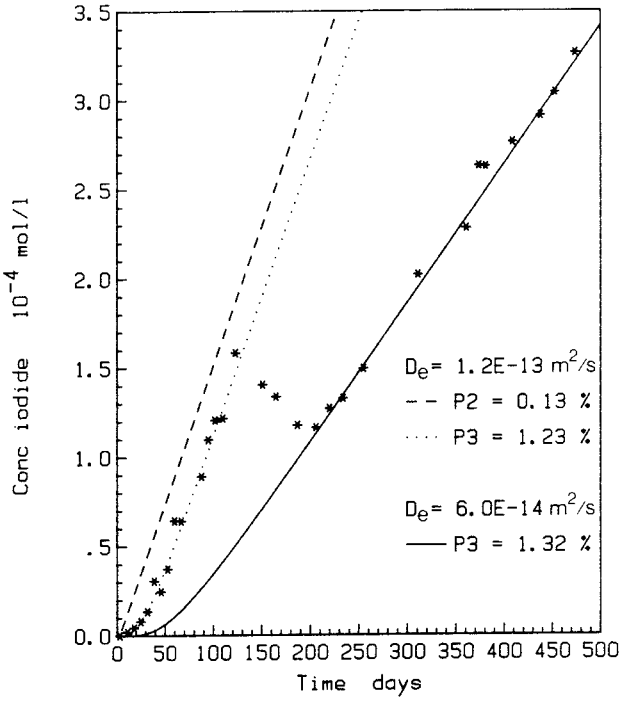

SS2: 1

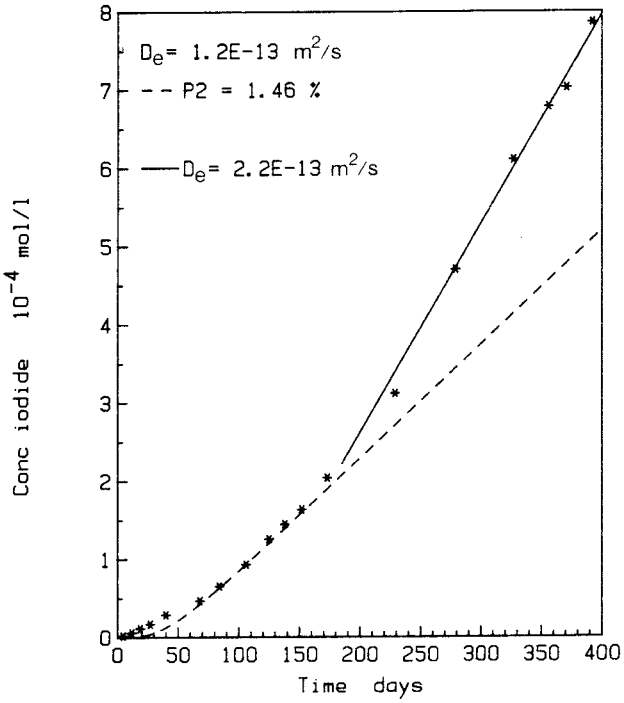

SS2: 2

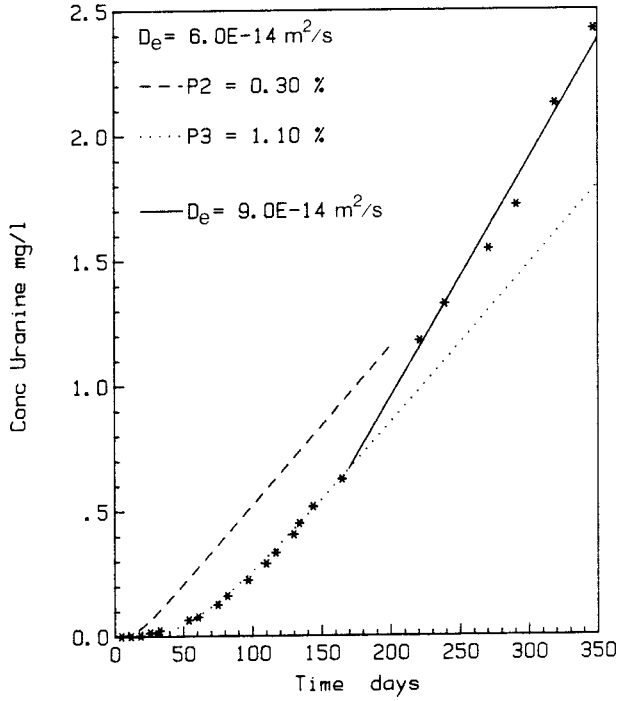

FI 81:1

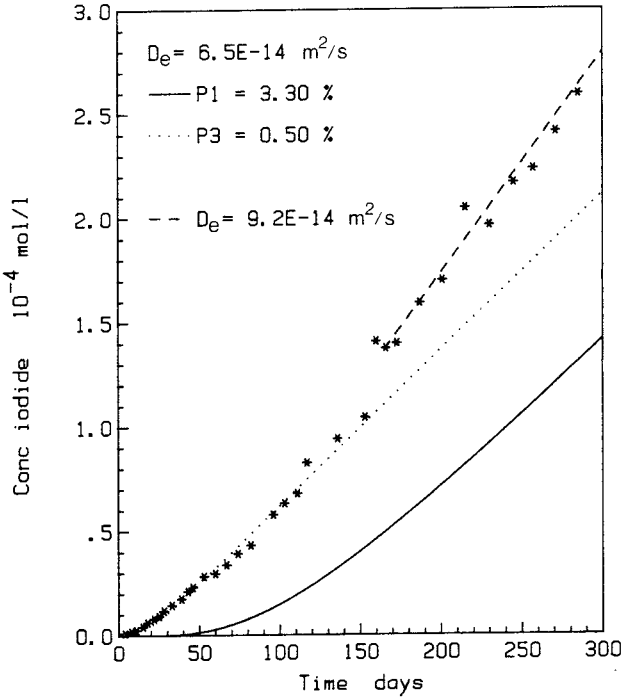

FI 81:2

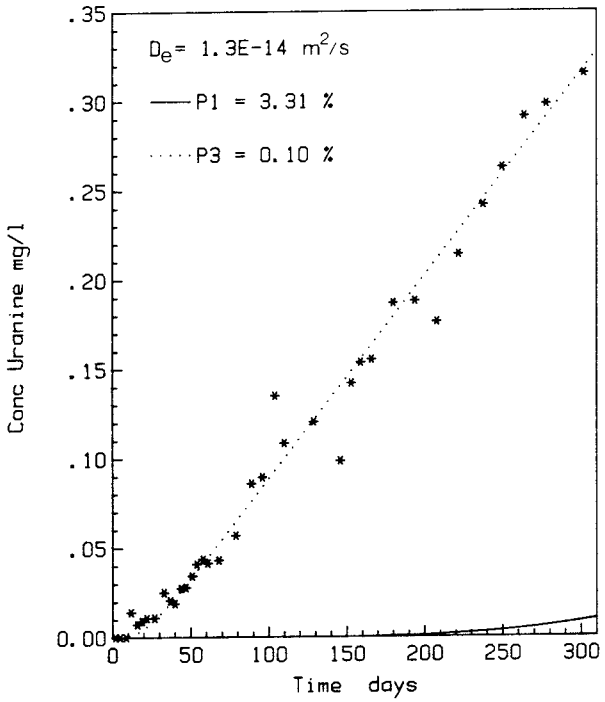

FI 83:1

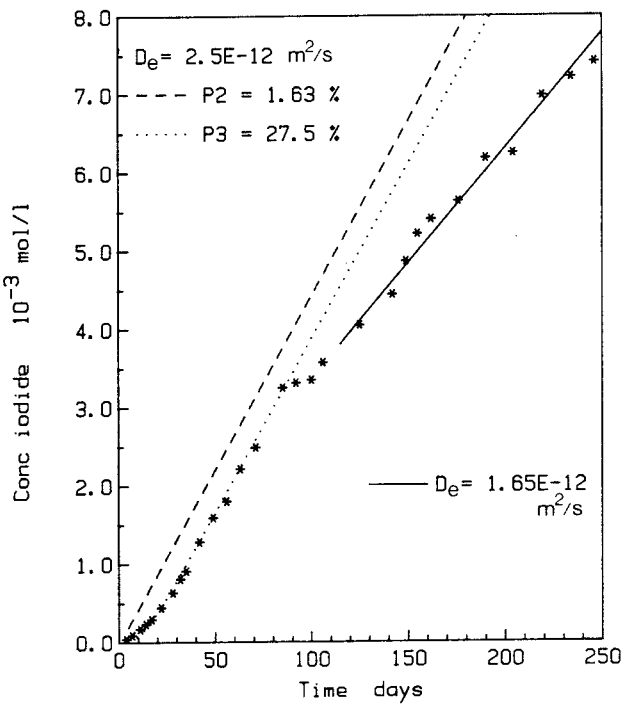

FI 83:2

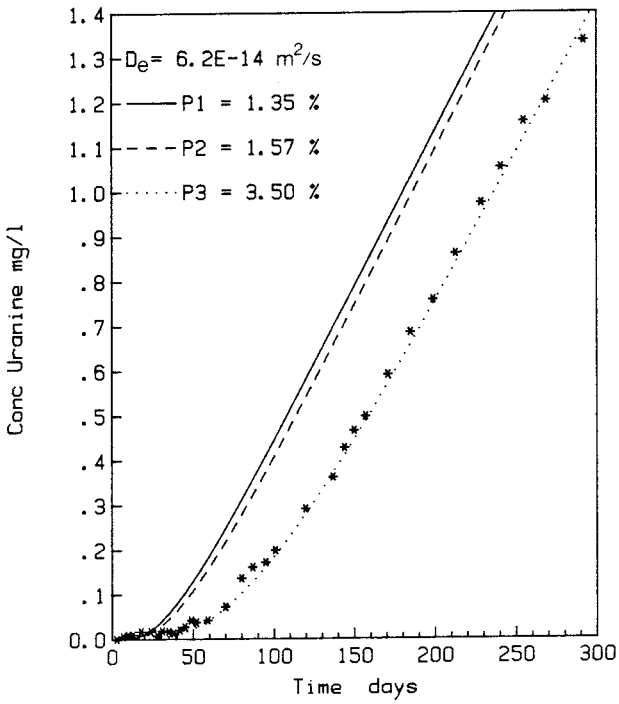

FI 85: 1

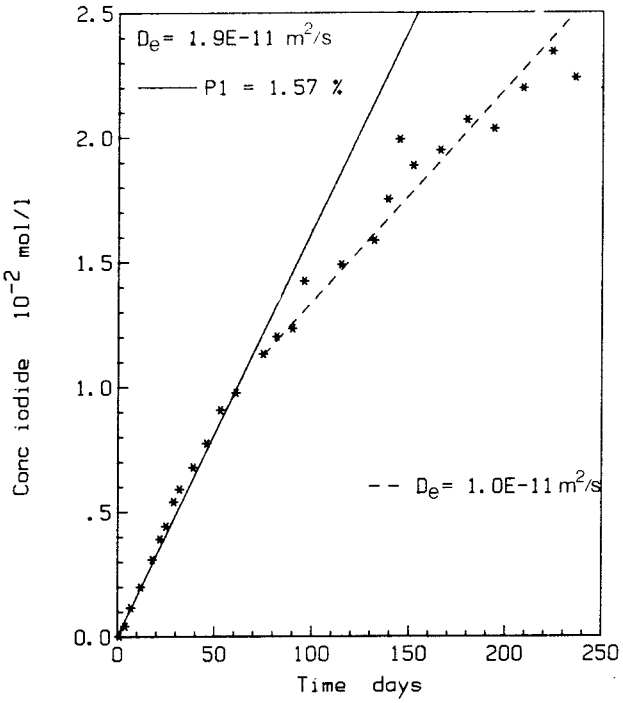

FI 85: 2

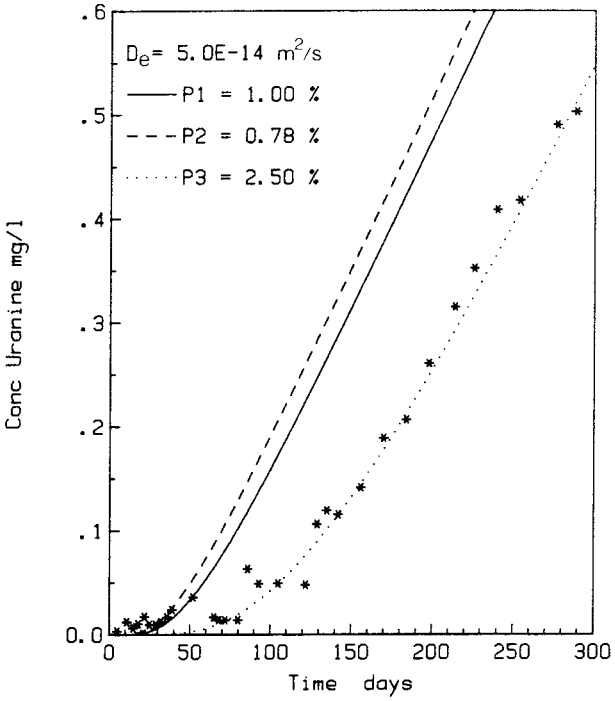

FI 41: 1

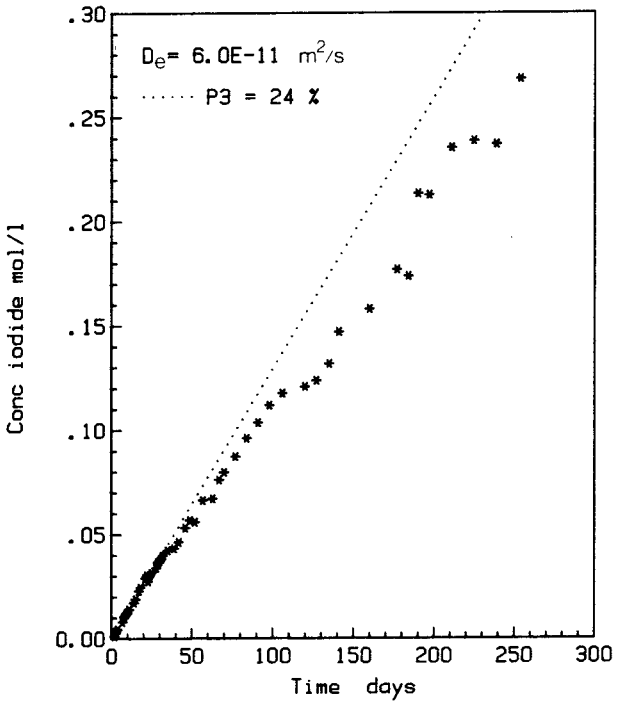

FI 41: 2

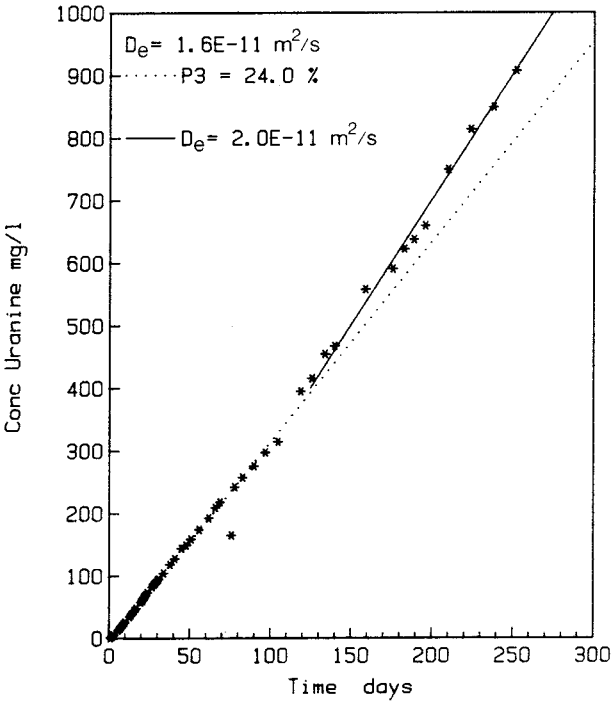

FI 41:3

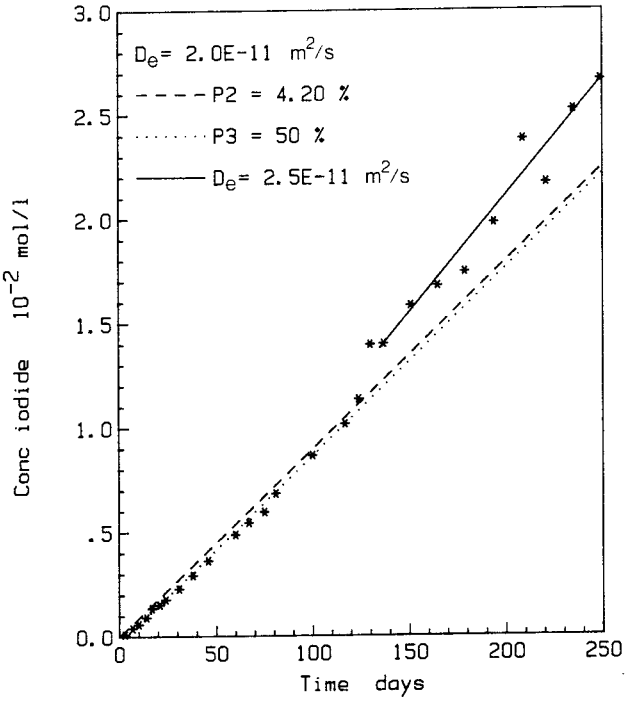

FI 41:4

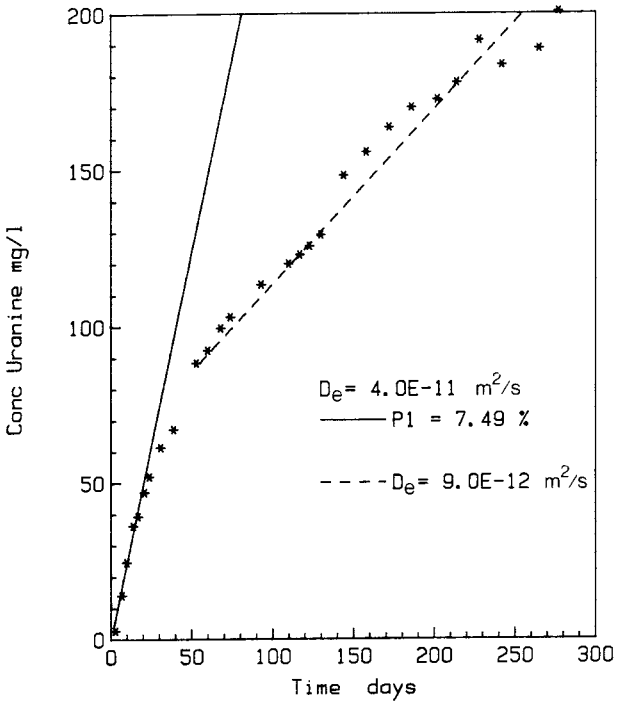

FI 51:1

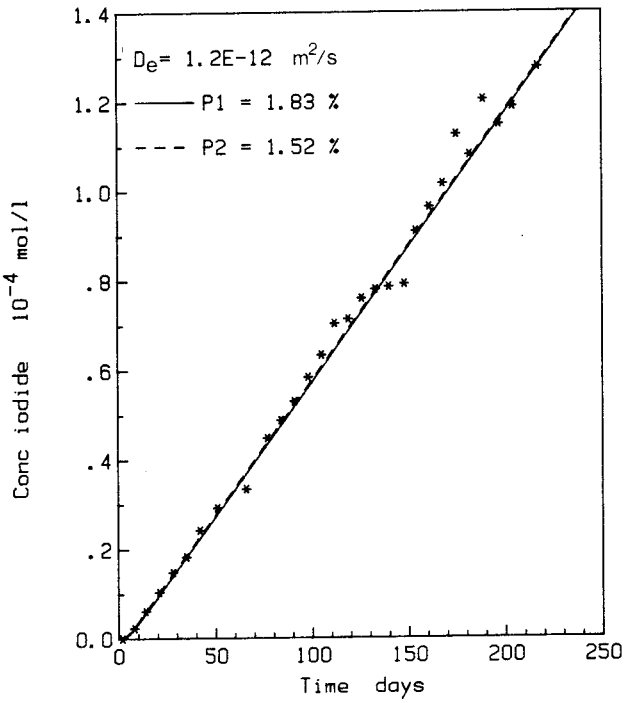

FI 51:2

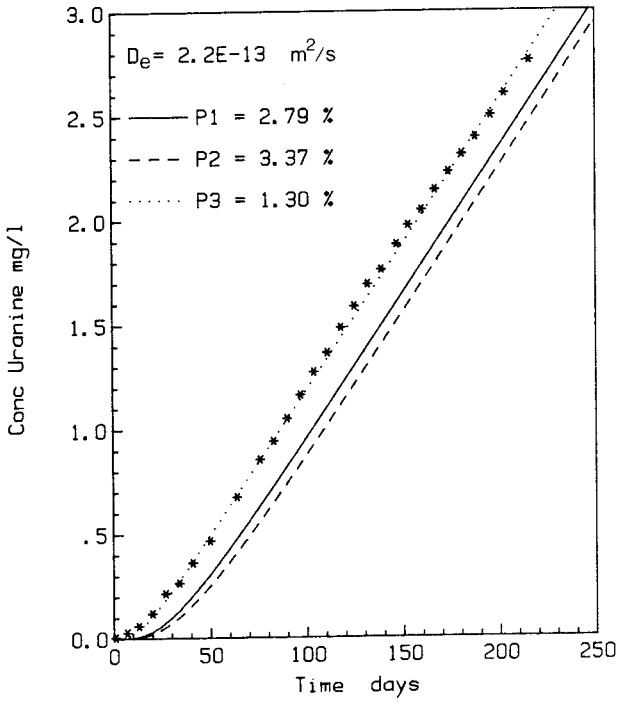

FI 51:3

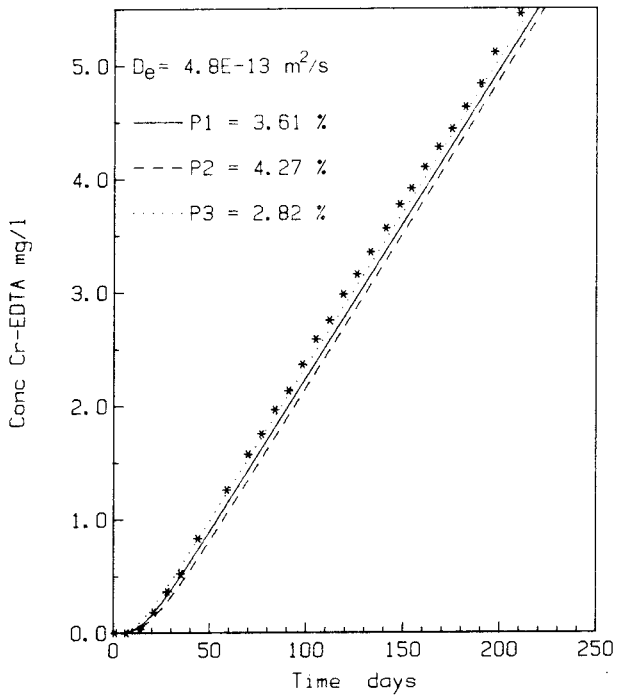

FI 87:1

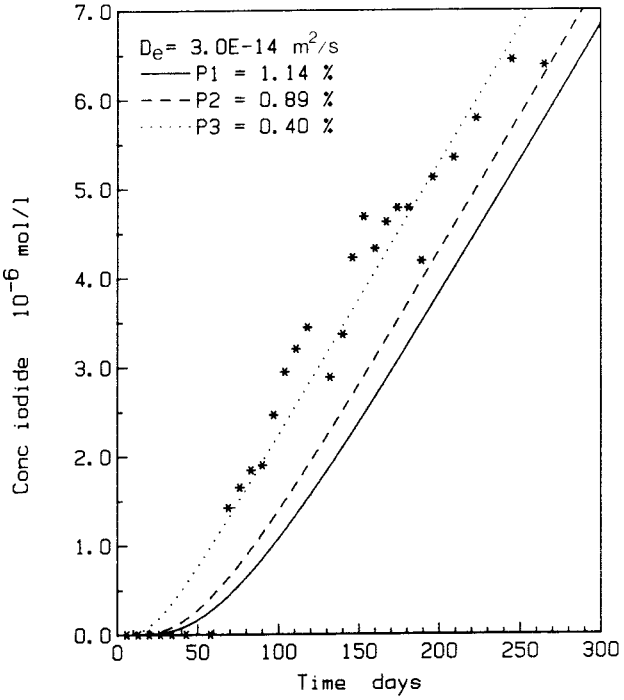

FI 87:2

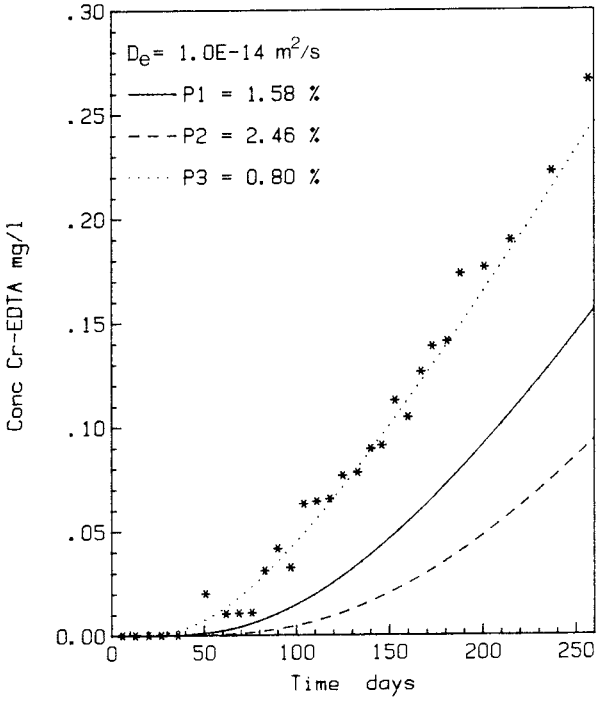

FI 87:3

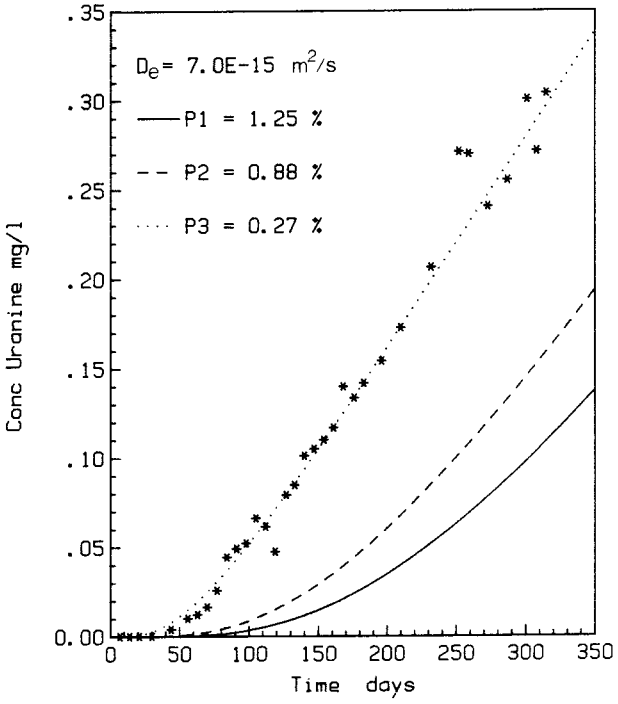

FI 71:1

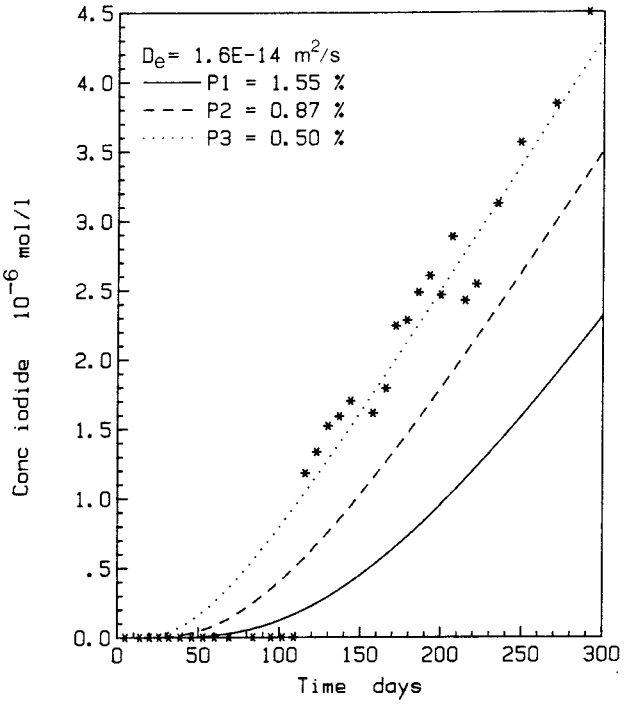

FI 71:2

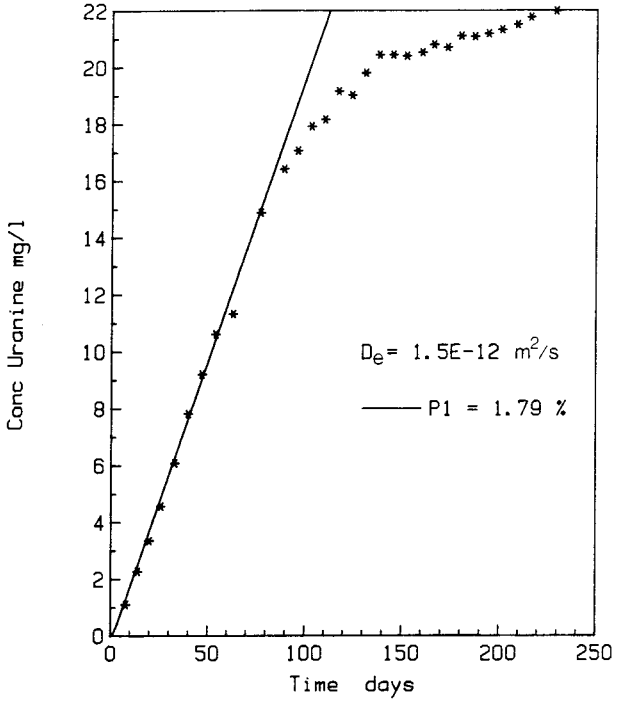

FI 71:3

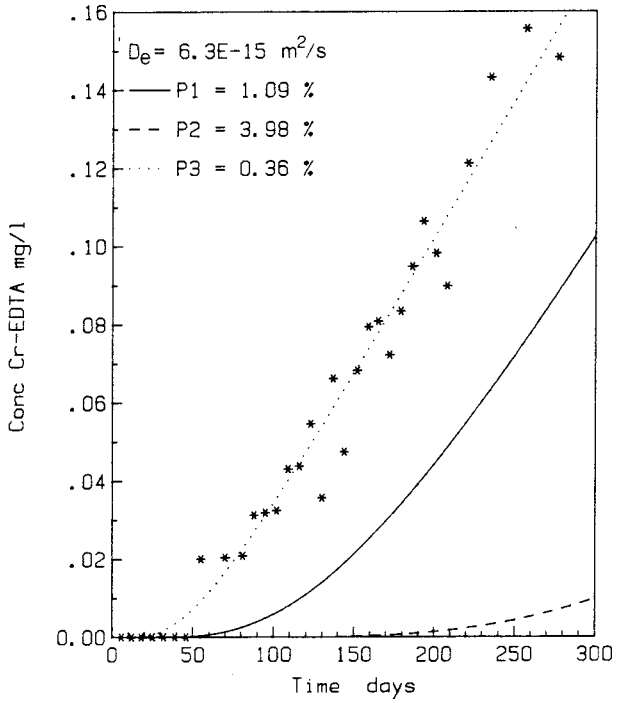

FI 88:1

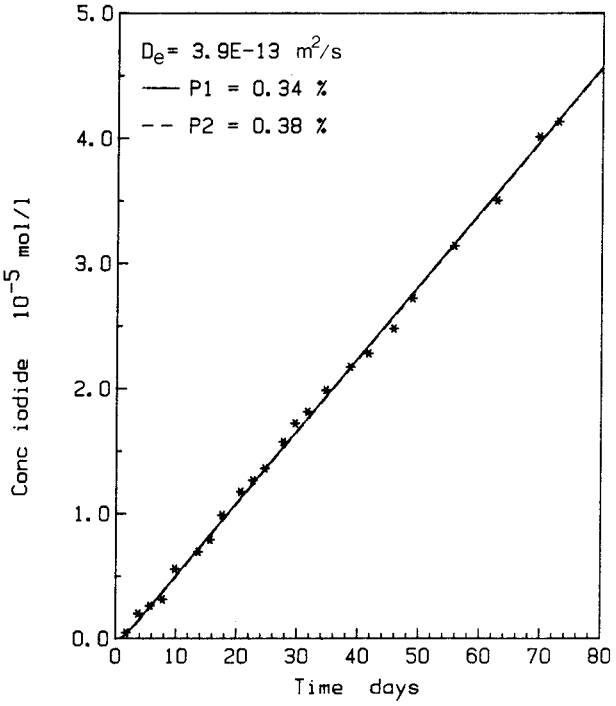

FI 88: 2

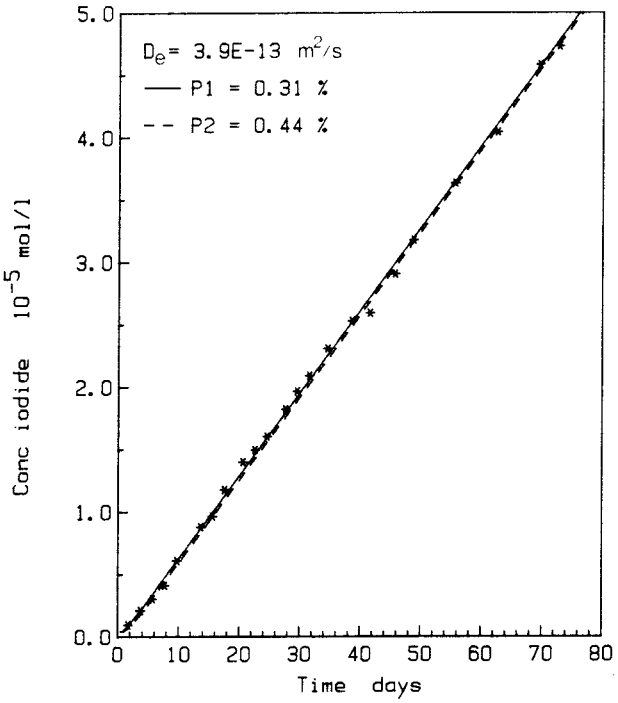

FI 88: 3

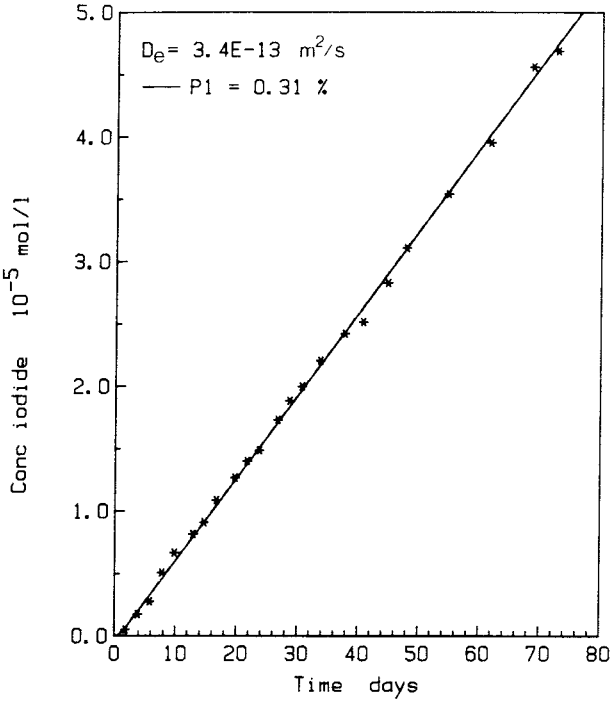

FI 88: 4

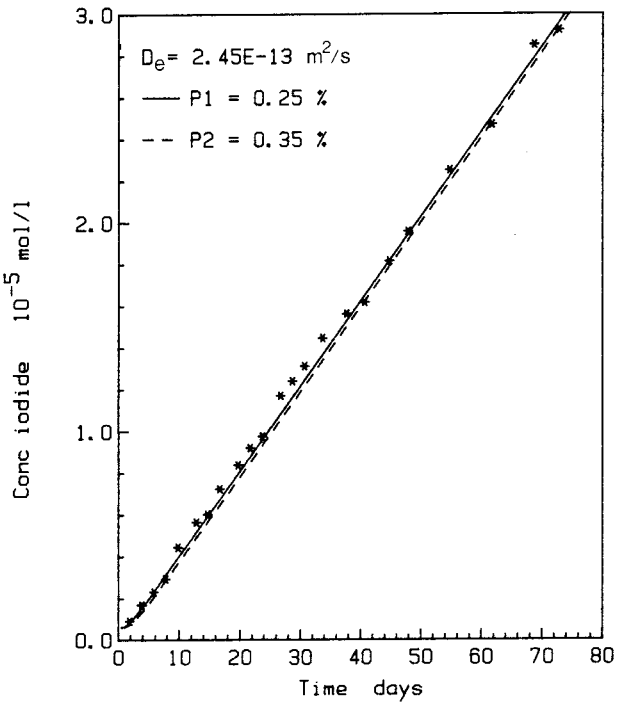

FI 88: 5

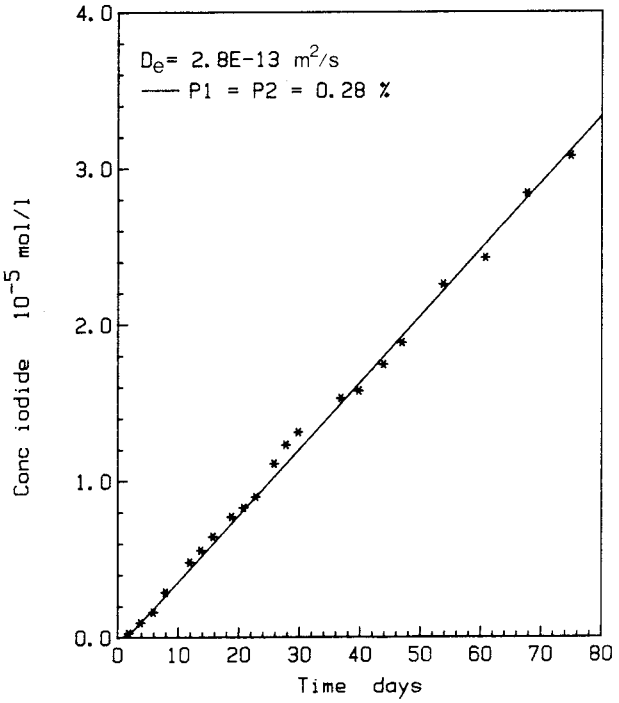

FI 88:6

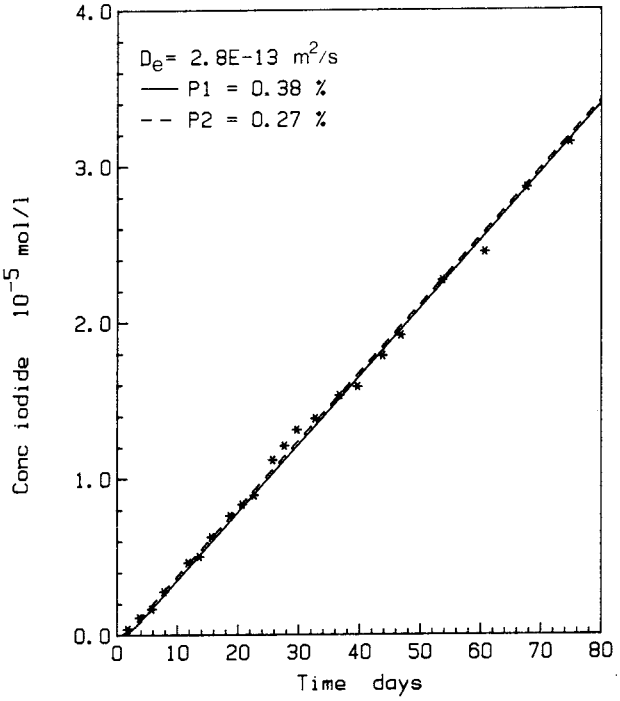

FI 88:7

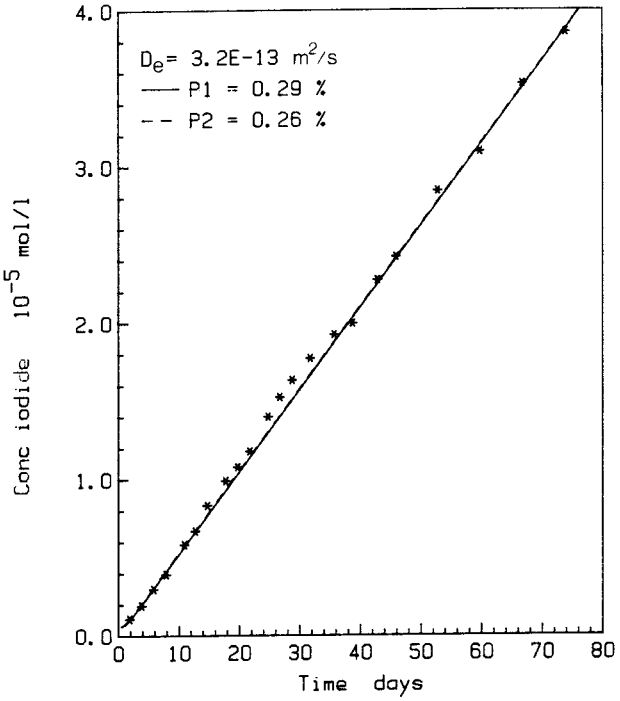

FI 88:8

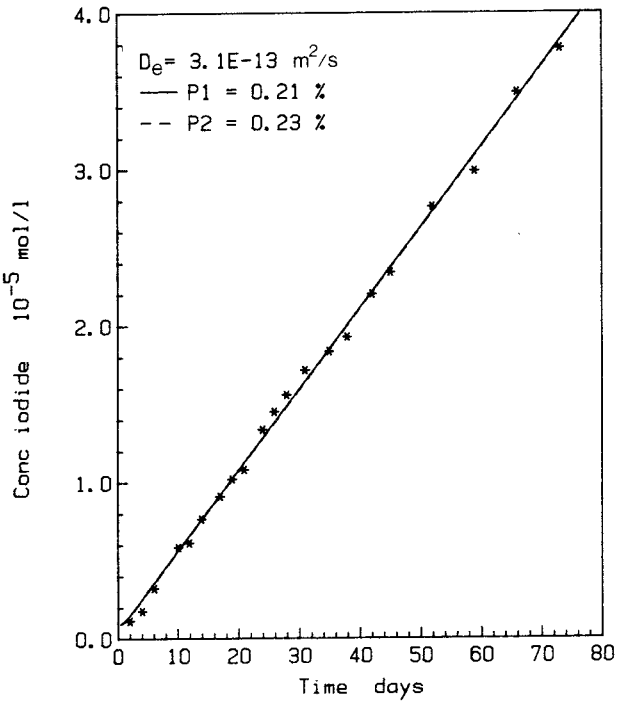

FI 88:9

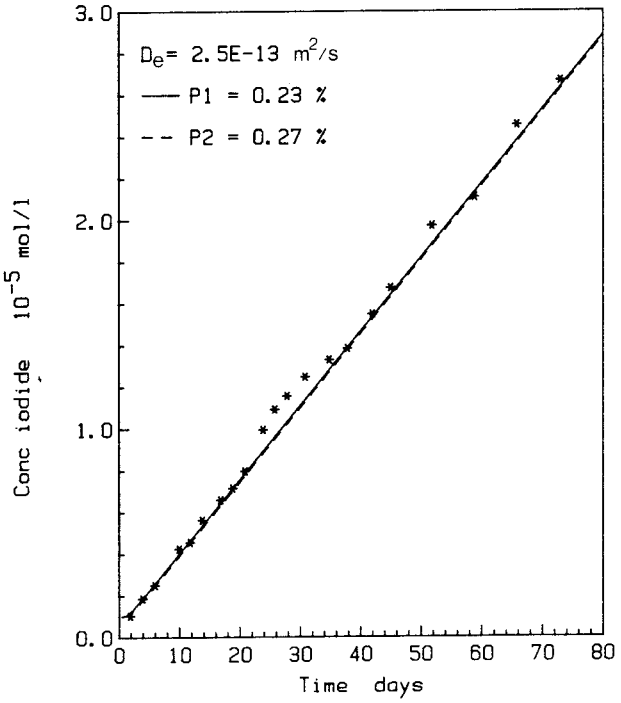

FI 89: 1

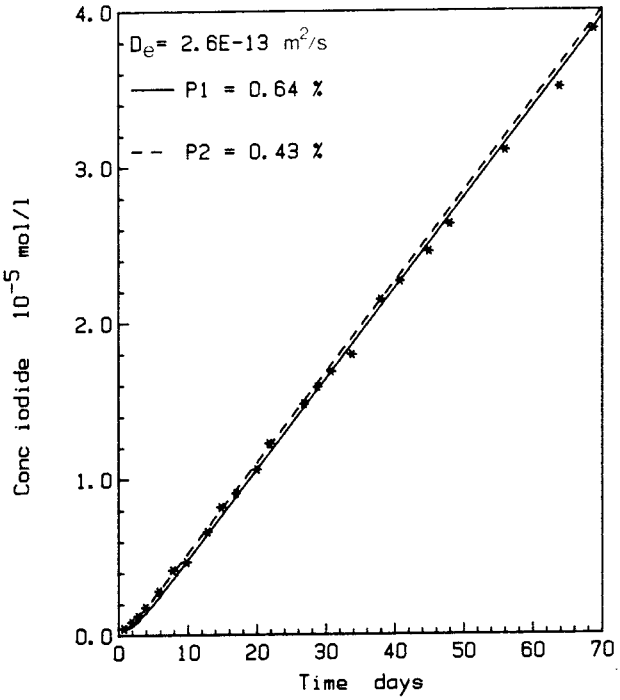

FI 89: 2

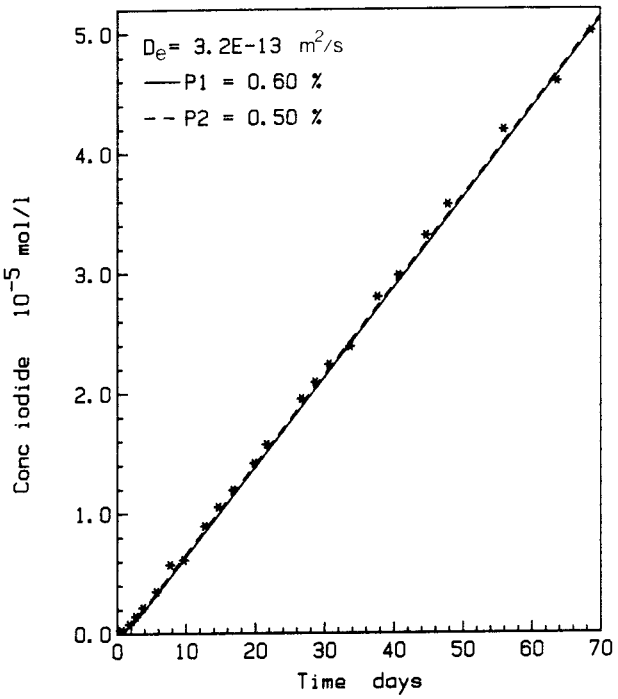

FI 89: 3

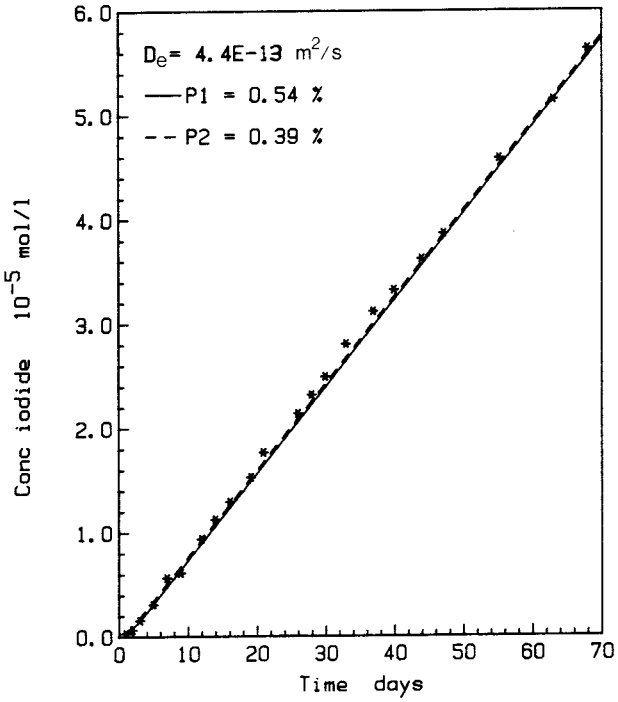

FI 89: 4

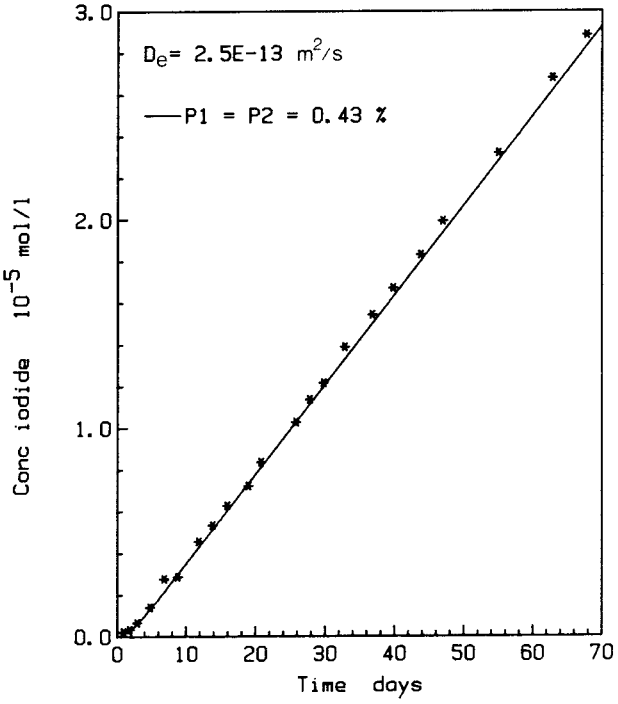

FI 89: 5

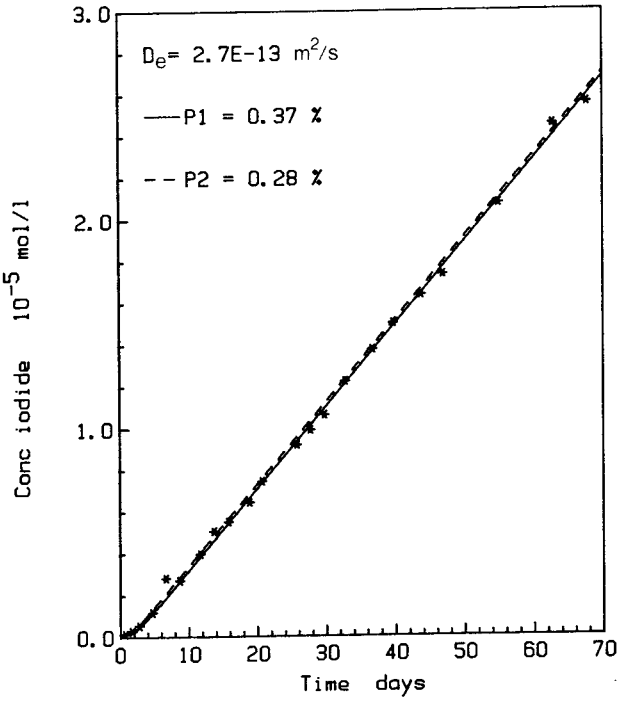

FI 89: 6

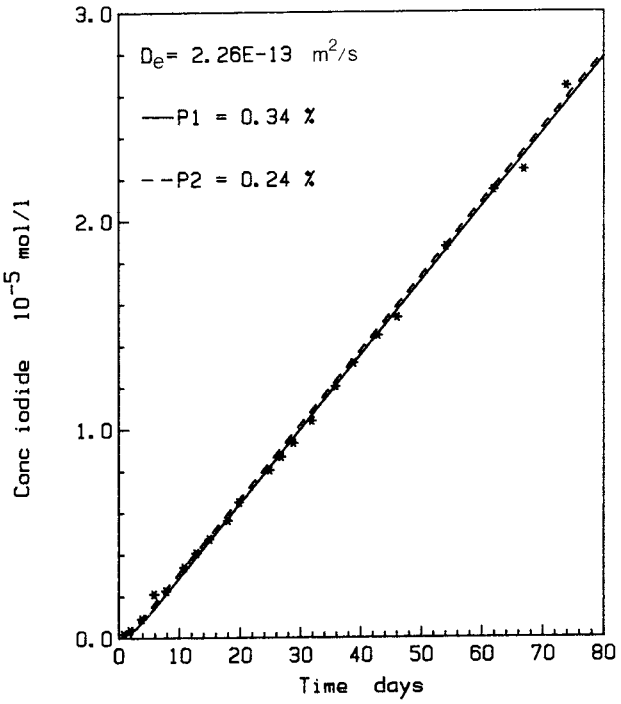

FI 89: 7

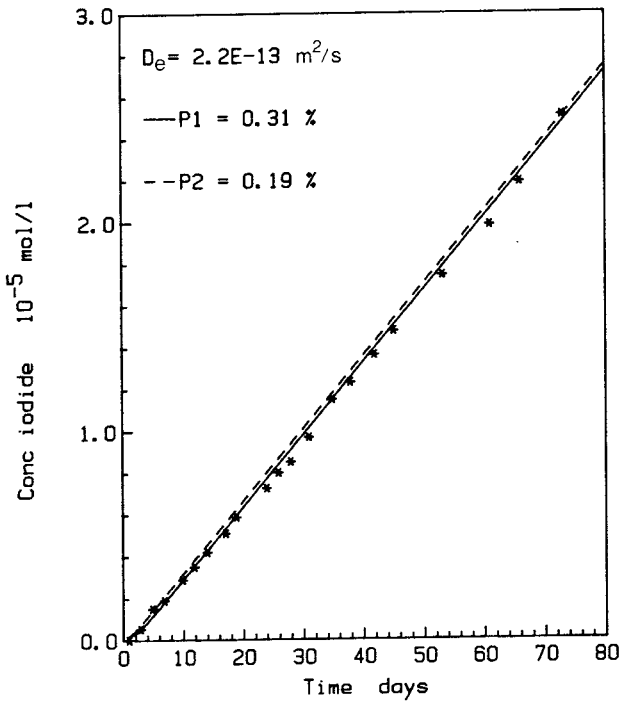

FI 89: 8

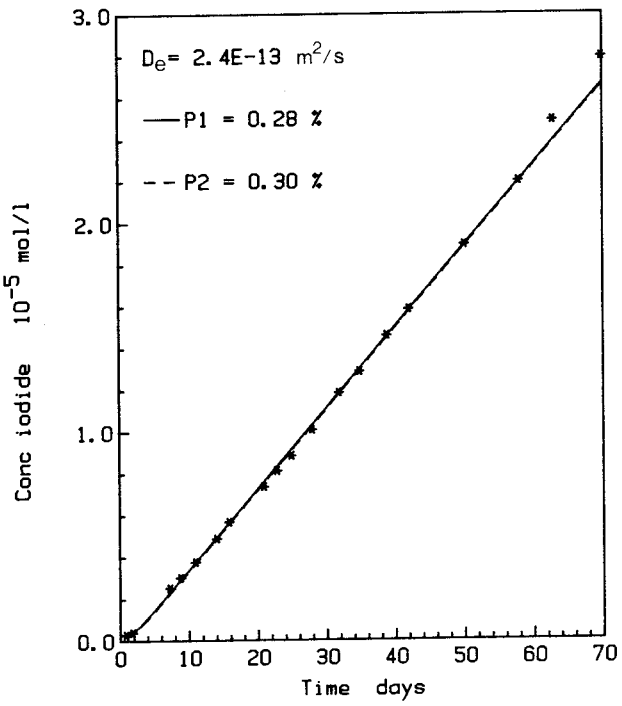

FI 89: 9

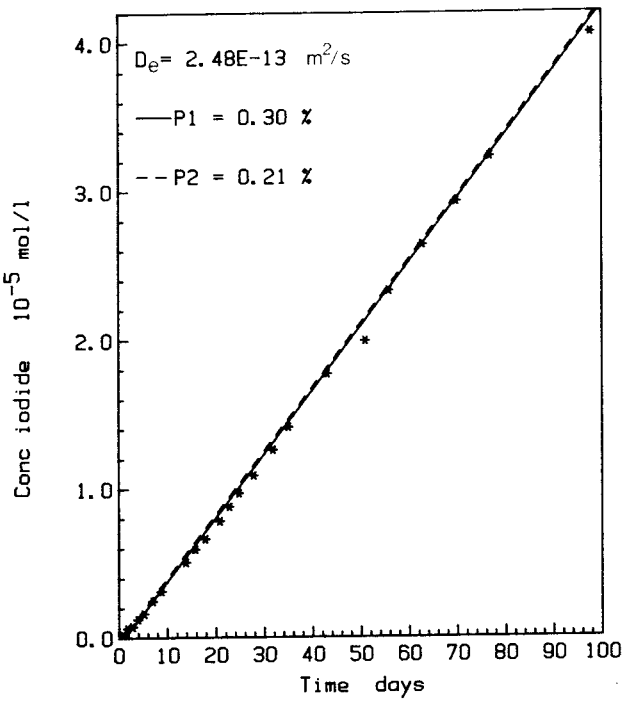

FI 89: 10

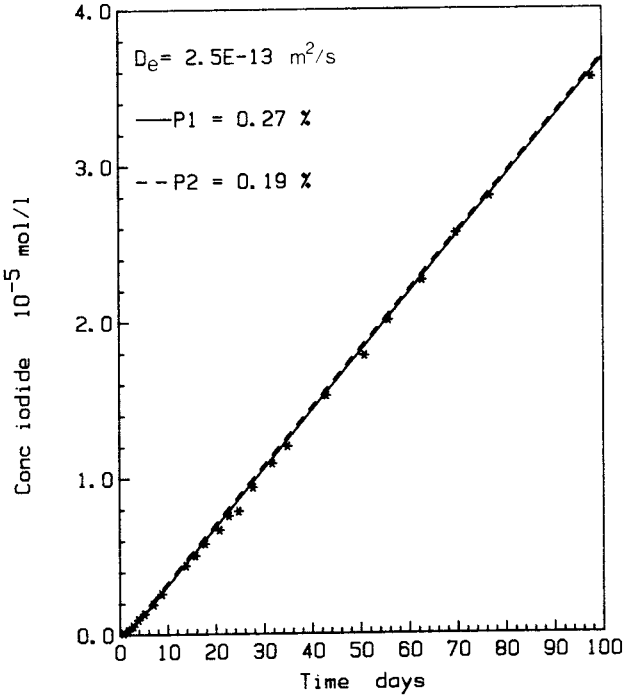

FI 89: 11

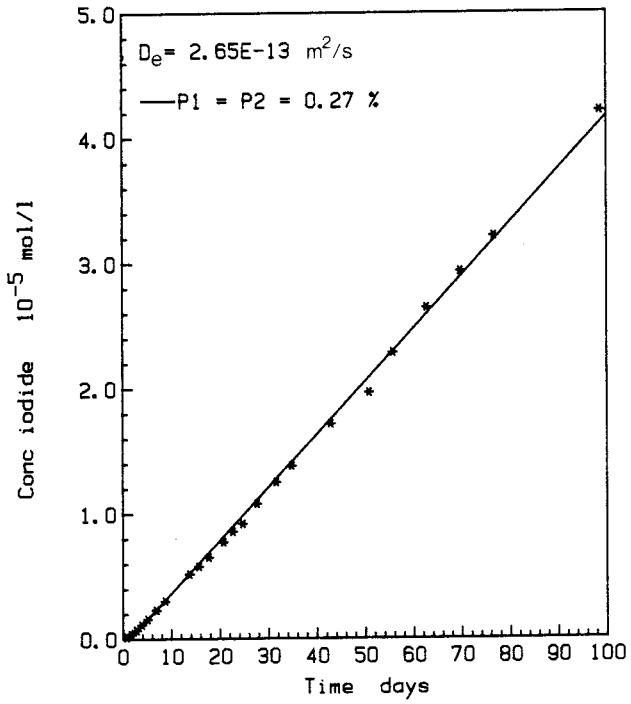

FI 89: 12

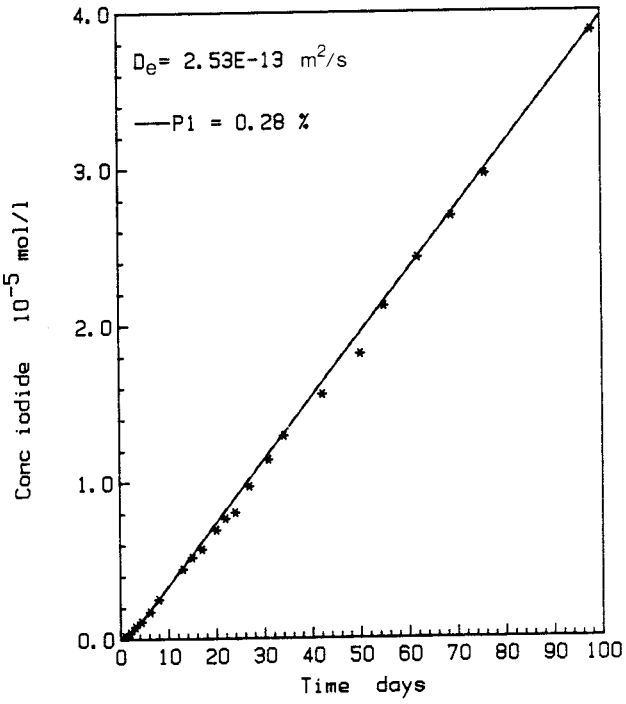

FI 89: 13

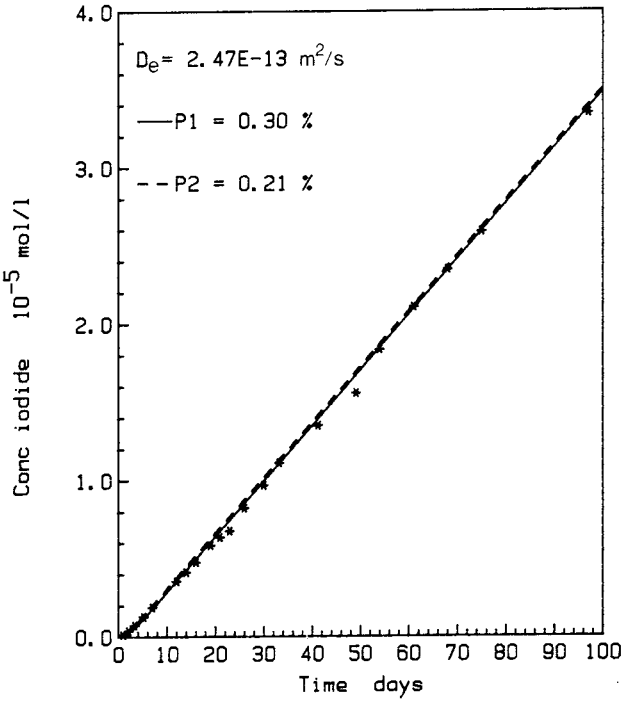

FI 89: 14

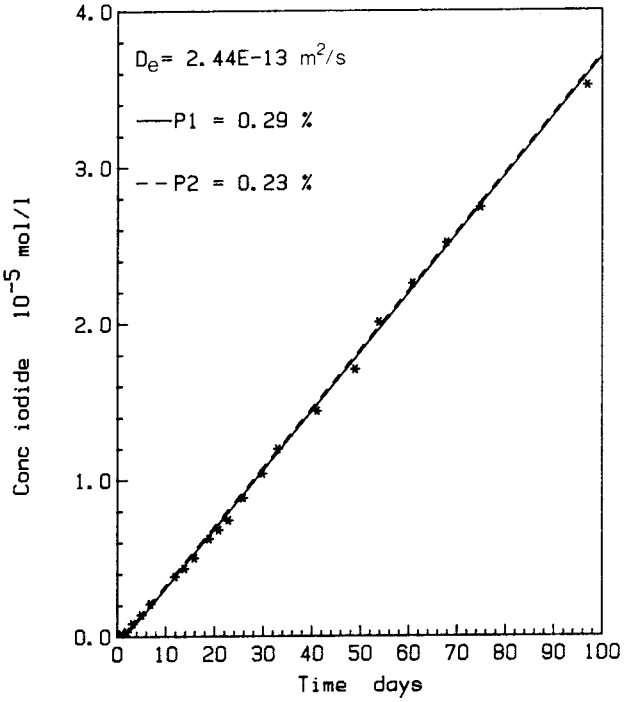

FI 89: 15

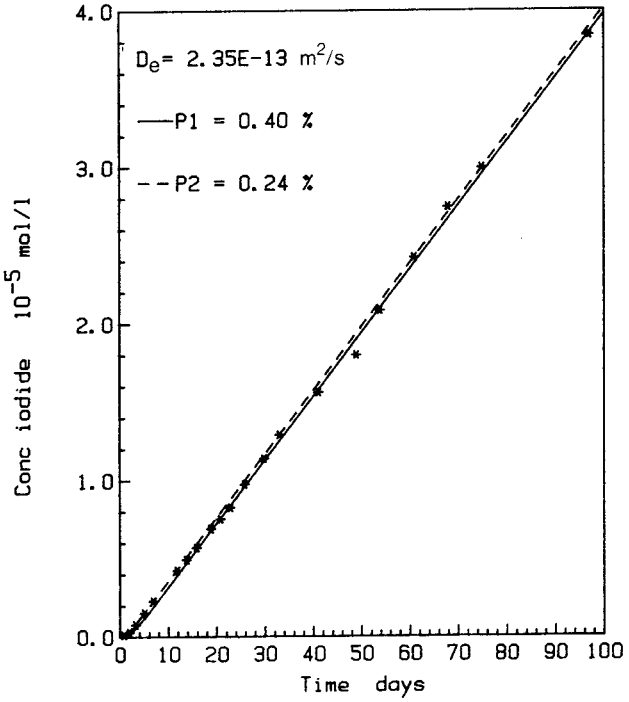

FI 89: 16

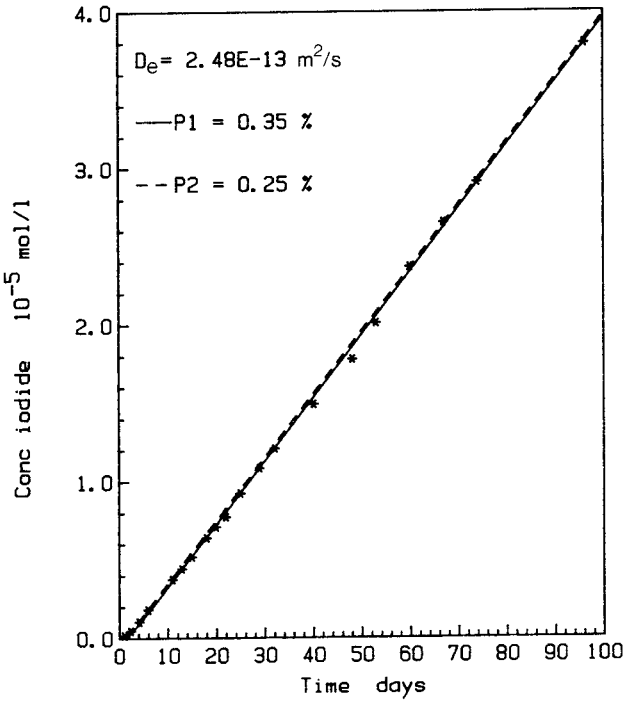

FI 89: 17

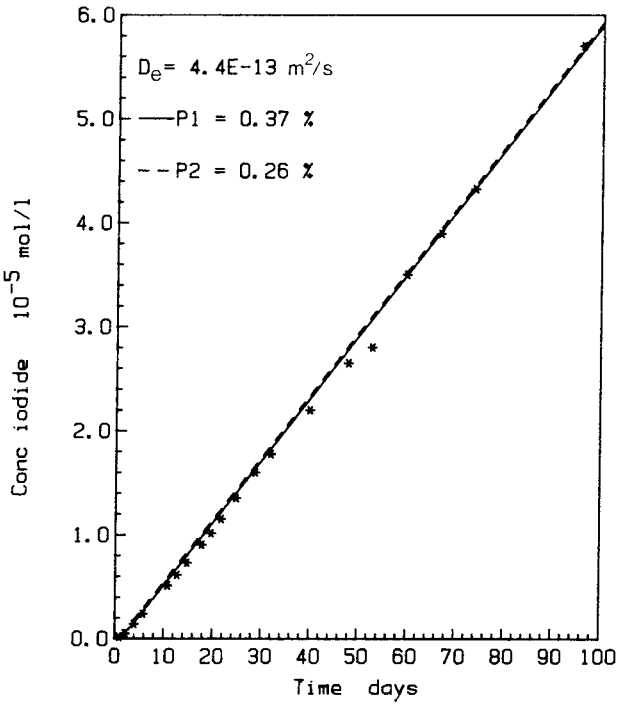
D_e= 4.4E-13 m^2/s
——P1 = 0.37 %
– – P2 = 0.26 %
Conc iodide 10^{-5} mol/l
Time days
0.0
1.0
2.0
3.0
4.0
5.0
6.0
0
10
20
30
40
50
60
70
80
90
100

List of Technical Reports

1977–78
TR 121
KBS Technical Reports 1 – 120.
Summaries. Stockholm, May 1979.

1979
TR 79–28
The KBS Annual Report 1979.
KBS Technical Reports 79-01 – 79-27.
Summaries. Stockholm, March 1980.

1980
TR 80–26
The KBS Annual Report 1980.
KBS Technical Reports 80-01 – 80-25.
Summaries. Stockholm, March 1981.

1981
TR 81–17
The KBS Annual Report 1981.
KBS Technical Reports 81-01 – 81-16.
Summaries. Stockholm, April 1982.

1982
TR 82–28
The KBS Annual Report 1982.
KBS Technical Reports 82-01 – 82-27.
Summaries. Stockholm, July 1983.

1983
TR 83–77
The KBS Annual Report 1983.
KBS Technical Reports 83-01 – 83-76
Summaries. Stockholm, June 1984.

1984
TR 85–01
Annual Research and Development Report 1984
Including Summaries of Technical Reports Issued during 1984. (Technical Reports 84-01– 84-19)
Stockholm June 1985.

1985
TR 85–01
Annual Research and Development Report 1984
Including Summaries of Technical Reports Issued during 1984.
Stockholm June 1985.

TR 85–02
The Taavinunnanen gabbro massif. A compilation of results from geological, geophysical and hydrogeological investigations.
Bengt Gentzschein
Eva-Lena Tullborg
Swedish Geological Company
Uppsala, January 1985